The BLAST Detector

John Calarco - University of New Hampshire

HUGS – June, 2006

Outline

- Scientific motivation
- BLAST program
- Stored beam and Compton polarimeter
- Internal target in the stored beam
- The BLAST detector
- Detector performance

Introduction

- Matter is made of atoms…

- The heart of the atom is the nucleus

- Nuclei contain protons and neutrons – or collectively, nucleons

- Goals are to test theories of nuclear and nucleon structure

- What is the nature of the NN interaction?

-How do we describe nuclear

and nucleon structure?

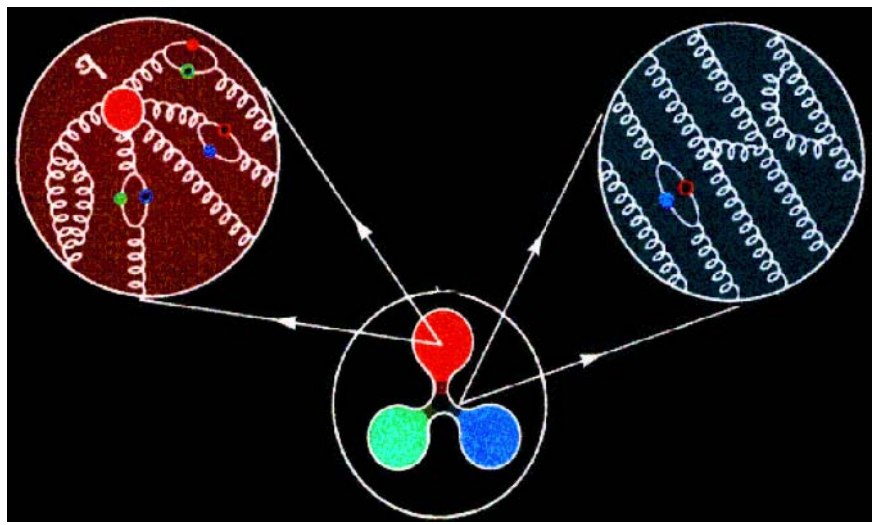

Introduction

Bates Large Acceptance Spectrometer Toroid

- Symmetric, large acceptance, general purpose detector
- Polarized electron beam in storage ring (SHR)
  850 MeV, 200 mA, $P_e = 65\%$ (longitudinal)
- Highly polarized, internal gas target of H and D (ABS)
  6×10^{13} atoms/cm^2, L $= 6\times10^{31}/(\text{cm}^2\text{s})$, $P_{H/D} = 80\%$,
  free spin orientation
- Study electromagnetic structure of the p, d, and n
  with spin-dependent inclusive and exclusive
  electron scattering at $Q^2 = 0.1{-}0.8$ (GeV/c)^2

Approved BLAST Scientific Program

Form Factor Measurements: $Q^2 \leq 1.0$ (GeV/c)^2

Proton Charge and Magnetism

- Elastic Scattering with Polarized Beam and *H* Target (**01-01**)

Neutron Charge and Magnetism and Deuteron Electromagnetic Structure

- Quasi-elastic Scattering with Polarized Beam and *D* Target (**89-12** and **91-09**)
- Elastic scattering off Tensor and Vector Polarized Deuterium (**00-03 and 03-02**)

BLAST - Underlying Idea

- Capitalize on the magnetism of the nucleus

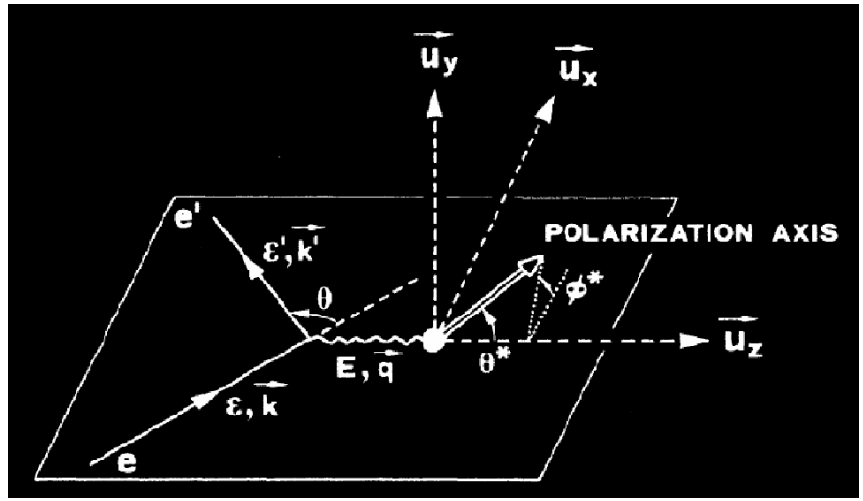

- We can polarize a collection of nuclei

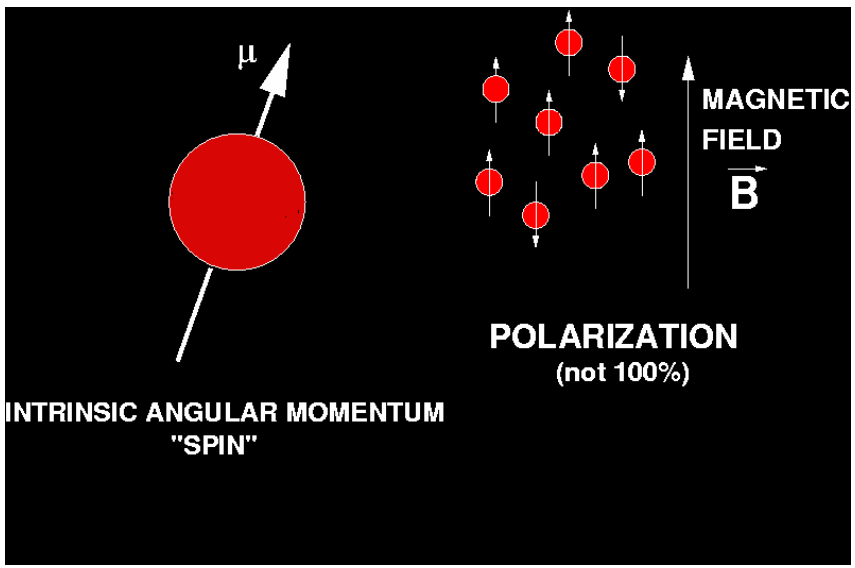

- Polarization observables will manifest themselves!

BLAST Physics Program

- High quality data for nucleon and deuteron structure by means of spin-dependent electron scattering

Pol. $\overrightarrow{H}$:	$\overrightarrow{p}(\vec{e},e')$	$\overrightarrow{p}(\vec{e},e'p)$	$\overrightarrow{p}(\vec{e},e'\pi^{+,0})$		
	Inclusive	G_E^p/G_M^p	N-Δ: C2/M1		
Vect.-Pol. $\overrightarrow{D}$:	$\overrightarrow{d}(\vec{e},e')$	$\overrightarrow{d}(\vec{e},e'd)$	$\overrightarrow{d}(\vec{e},e'p)$	$\overrightarrow{d}(\vec{e},e'n)$	$\overrightarrow{d}(\vec{e},e'\pi^{\pm,0})$
	G_M^n	T_{11}^e	A_{ed}^V	G_E^n	N-Δ
Tens.-Pol. $\overleftrightarrow{D}$:	$\overleftrightarrow{d}(e,e'd)$	$\overleftrightarrow{d}(e,e'p)$			
	T_{20}	A_d^T			

Bates Linac

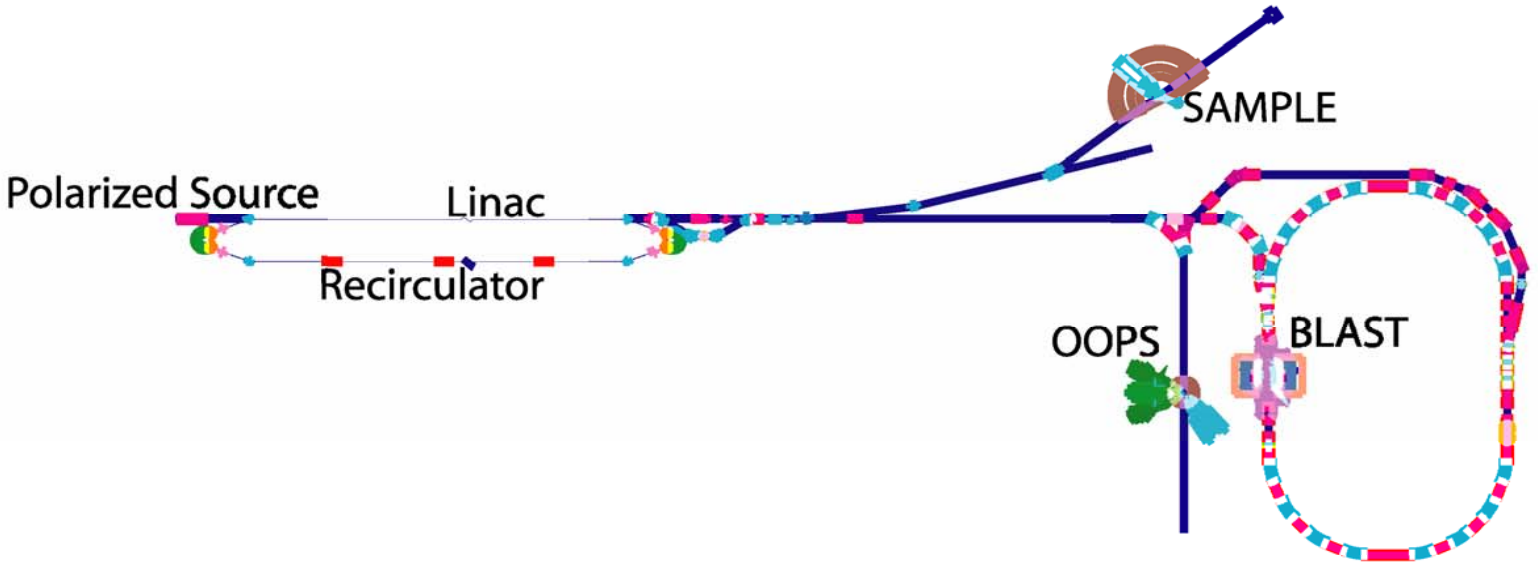

- **500MeV Linac recirculated to reach up to 1GeV**
- **Inject into South Hall Ring**
- **Polarization maintained by Siberian snakes**
- **Polarization monitored real time by Compton Polarimeter**
- **Internal Target located in the ring vacuum**

MIT-Bates Polarized Source

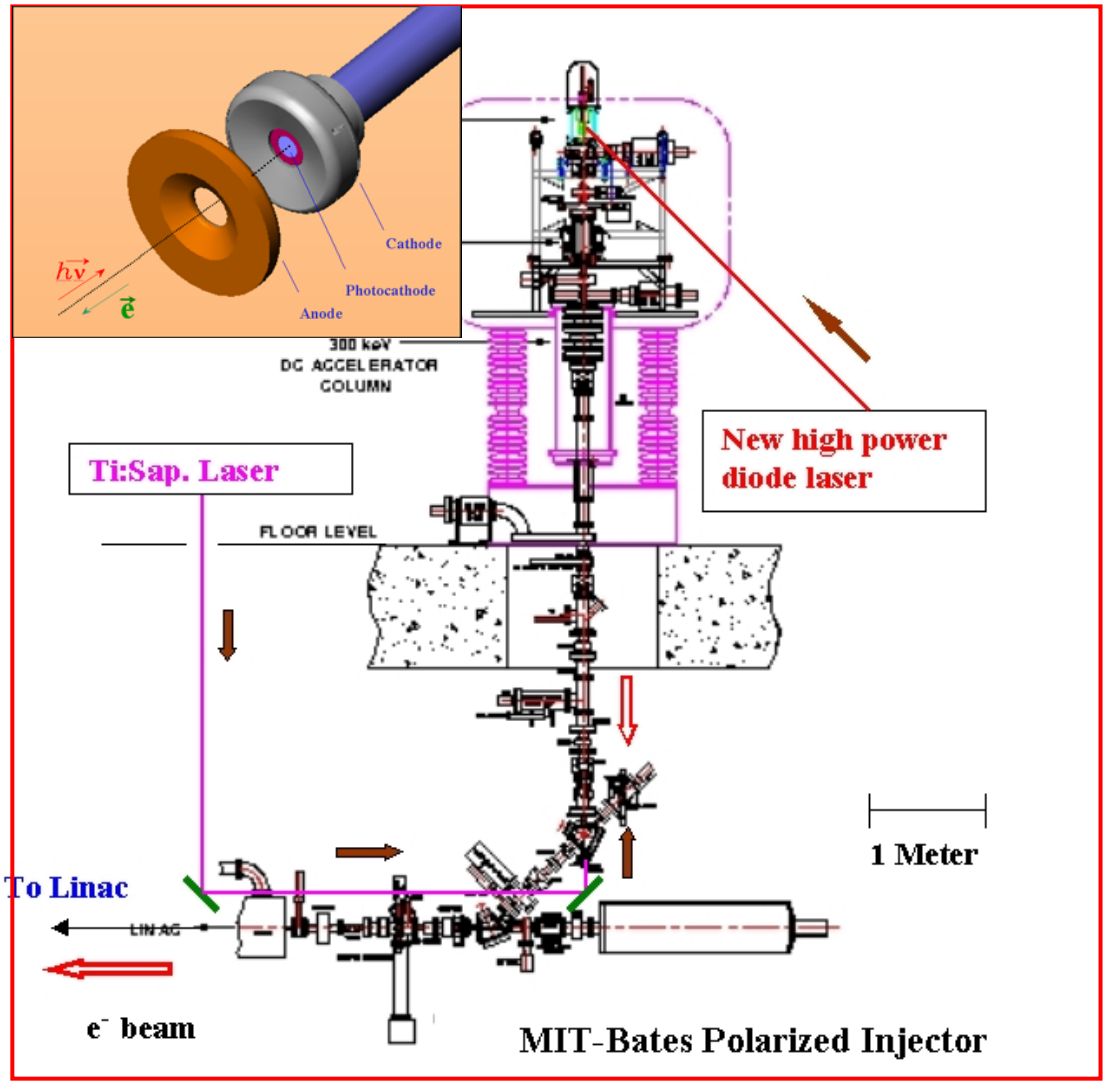

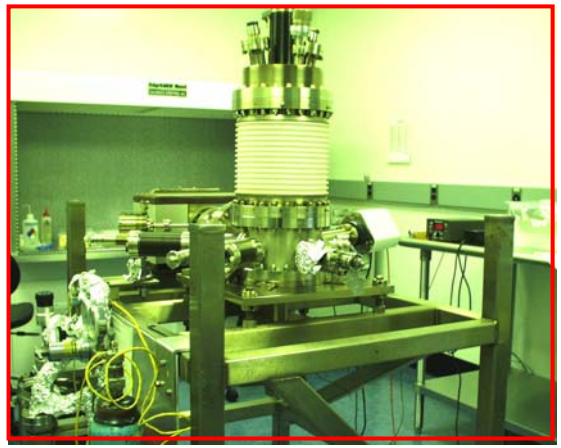

- Three identical guns:
  - injector
  - backup
  - test setup
- 4 days to interchange.

High Power diode laser for Bates polarized source

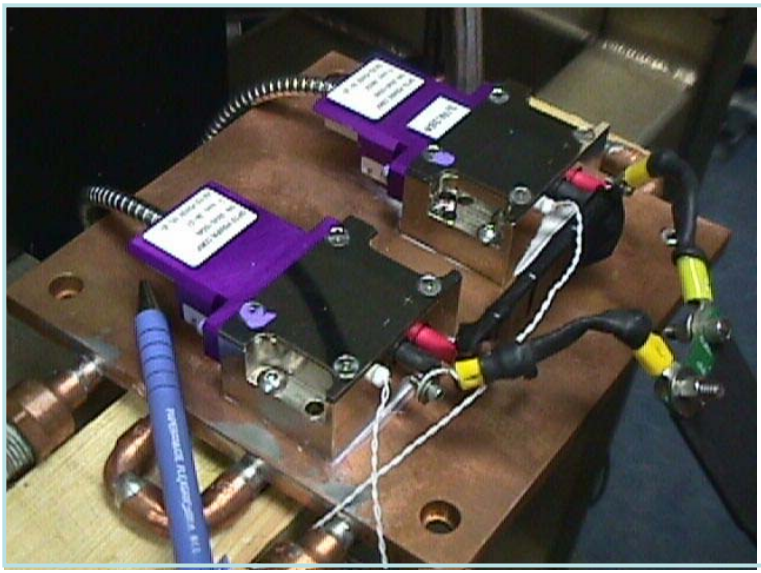

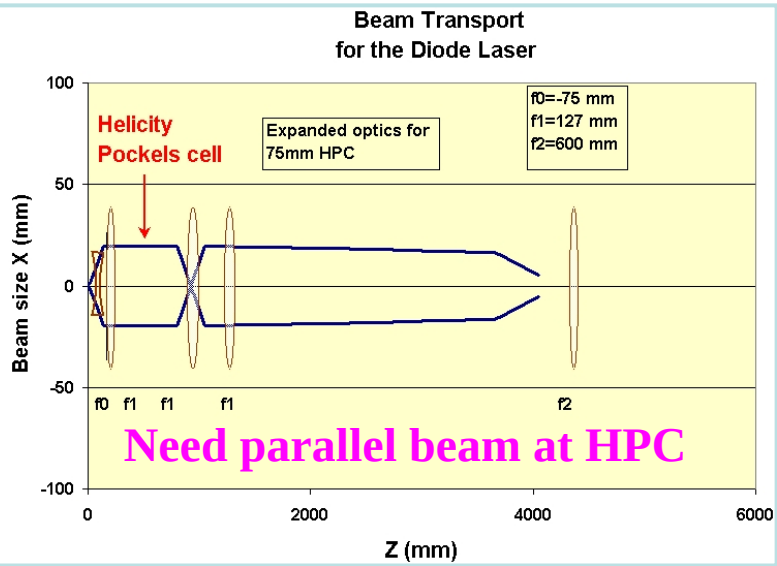

Fiber-coupled diode array lasers

- **wavelength:** 808± 3 nm (fixed) (need matching wafers)
- **emittance:** ~200 mm.mr ⟹ (short working distance)
- **power:** unpolarized: ~ 150 W pulsed 60 W CW
- **stability:** better than Ti:sapp laser by > 10
- **no correction Pockels cells needed.**
- **need large diameter optics (75 diameter HPC).**

MIT-Bates South Hall Ring

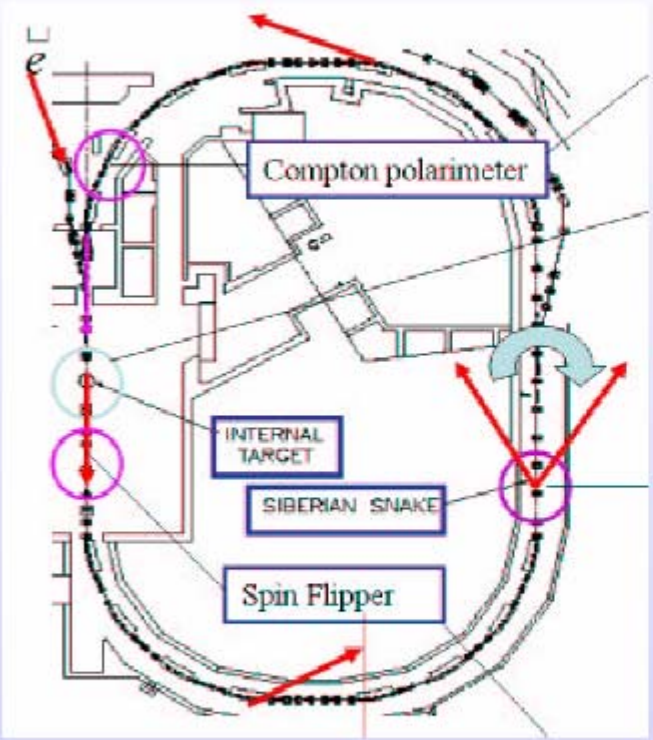

Monitoring of electron beam polarization

Injection with longitudinal spin at internal target

Siberian snake to restore longitudinal polarization

$< h > = 0.65 \pm 0.04$

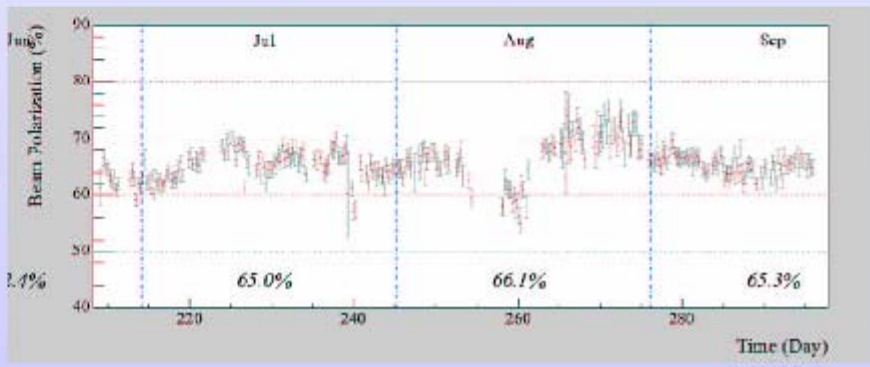

Polarization in Bates South Hall Ring

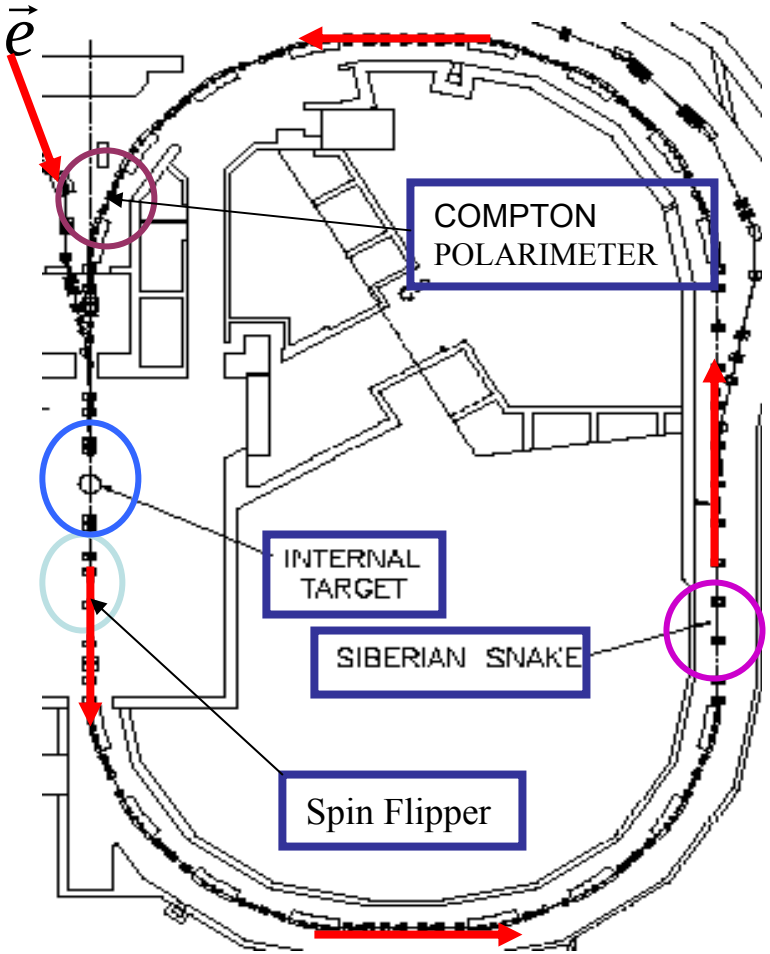

South Hall Ring

- Electrons injected with longitudinal polarization (controlled by Wien filter)
- Internal target inside BLAST Spectrometer
- Full Siberian Snake used to preserve polarization in Ring
- Compton polarimeter, separated from internal target by 22.5^{o} bend, measures longitudinal projection of beam polarization
- RF dipole to allow spin reversal with beam stored in Ring

Stored beam with injection currents up to 225 mA and lifetimes typically 20 – 30 minutes, monitored in real time

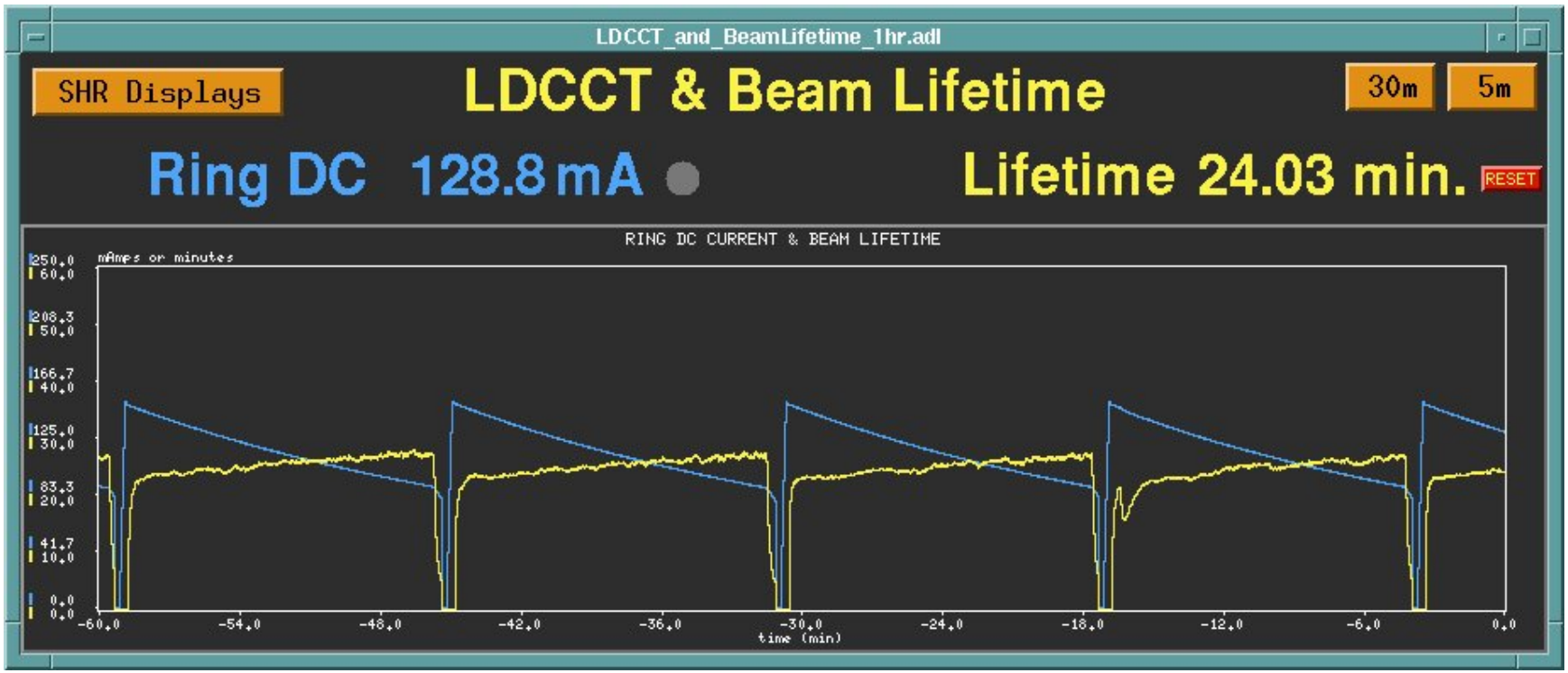

General Kinematics for Polarized *e* Scattering on a Polarized Target

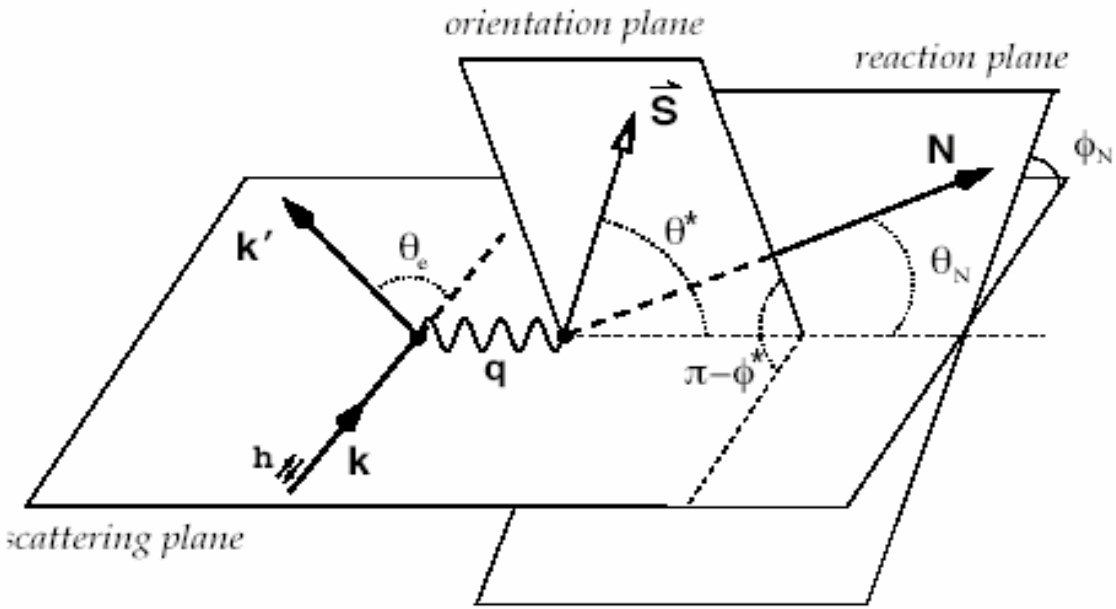

Compton Polarimetry Overview

• Laser backscattering provides a nondestructive means of sampling electrons from a high energy beam

• Compton scattering in highly relativistic frame compresses angular distribution into a narrow kinematic cone and shifts photon frequencies into gamma regime

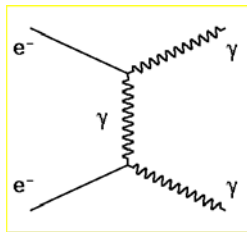

→ Detect backscattered photons with a compact detector

• Compton scattering cross section is well known theoretically and has a term dependent on electron spin and laser helicity

→ Can extract e^- polarization by measuring asymmetries in scattering rates for circularly polarized laser light

Compton Polarimetry Overview

- Compton scattering in highly relativistic frame compresses angular distribution into a narrow kinematic cone and shifts photon frequencies into gamma regime
  - > Detect backscattered photons with a compact detector
- Compton scattering cross section is well known theoretically and has a term dependent on electron spin and laser helicity
  - > Can extract e^- polarization by measuring asymmetries in scattering rates for circularly polarized laser light

Transverse polarization yields asymmetry in azimuthal distribution of scattered photons.
Longitudinal polarization yields asymmetry in scattered photon energy spectrum

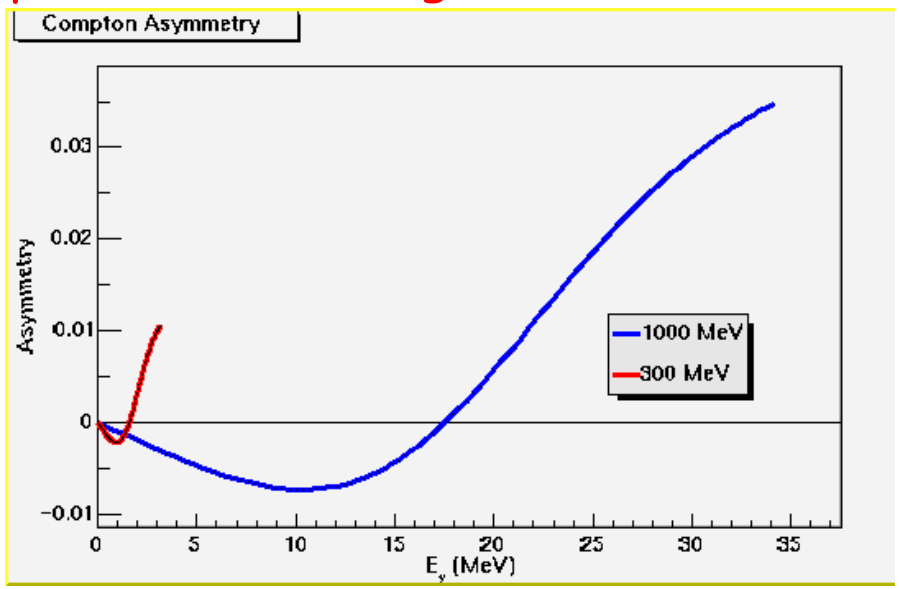

Compton Polarimetry Below 1 GeV

- Compton polarimetry is well established at high energy accelerators (A_{pol}~0.5)
- Different challenges exist in applying at energies below 1 *GeV.*
  - > Analyzing power falling with energy (A_{pol} < 0.05)
  - > Broader angular distribution for photons
  - > Background from low energy photons

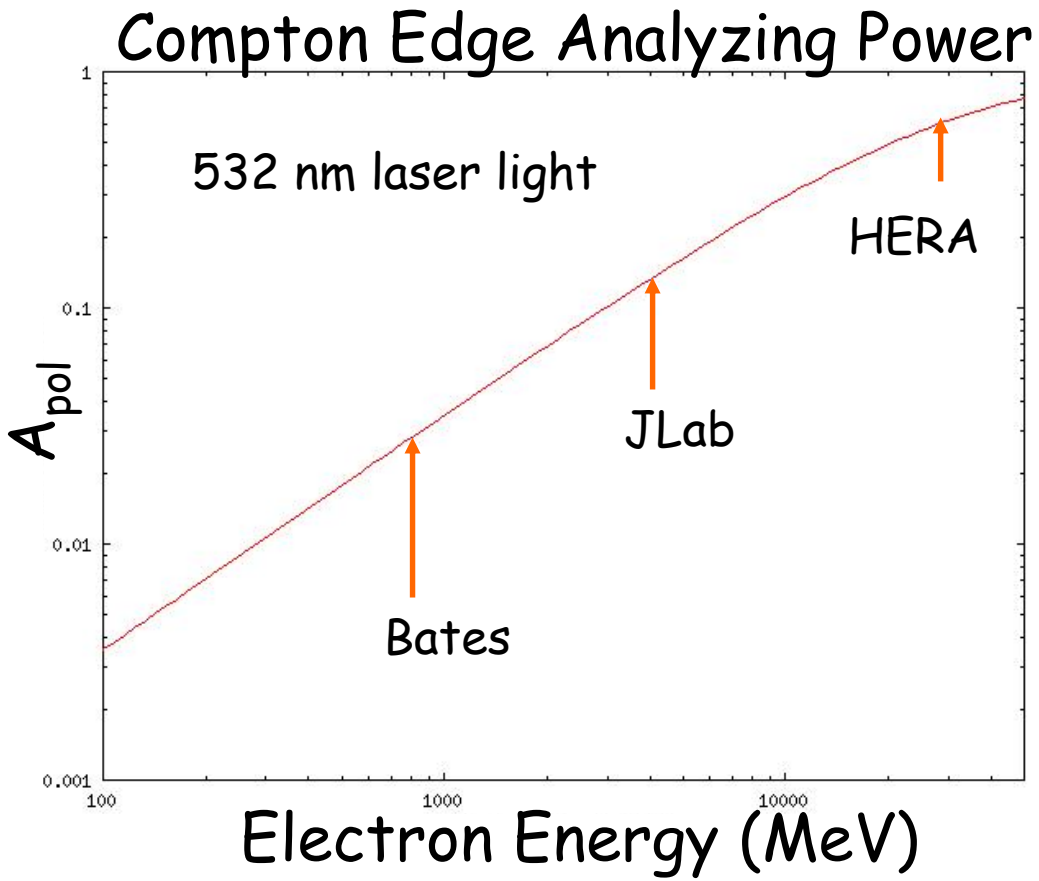

- Bates seeks precise polarization measurement for each ring fill (15 minutes) for experiments with BLAST.

SHR Compton Polarimeter

- Design based on NIKHEF Compton Polarimeter
- Compton polarimeter located upstream of BLAST target to reduce background, measures longitudinal projection of electron beam polarization
- Laser resides in shielded hut with 18 *m* flight path to Int. Region (IR)
- Laser trajectory varied remotely to overlap with electron beam in 4 *m* long straight section IR
- Photon calorimeter located 10 *m* from IR
- Tune electron beam first to align using bremsstrahlung background. Backscattered gamma trajectory defined by electron trajectory

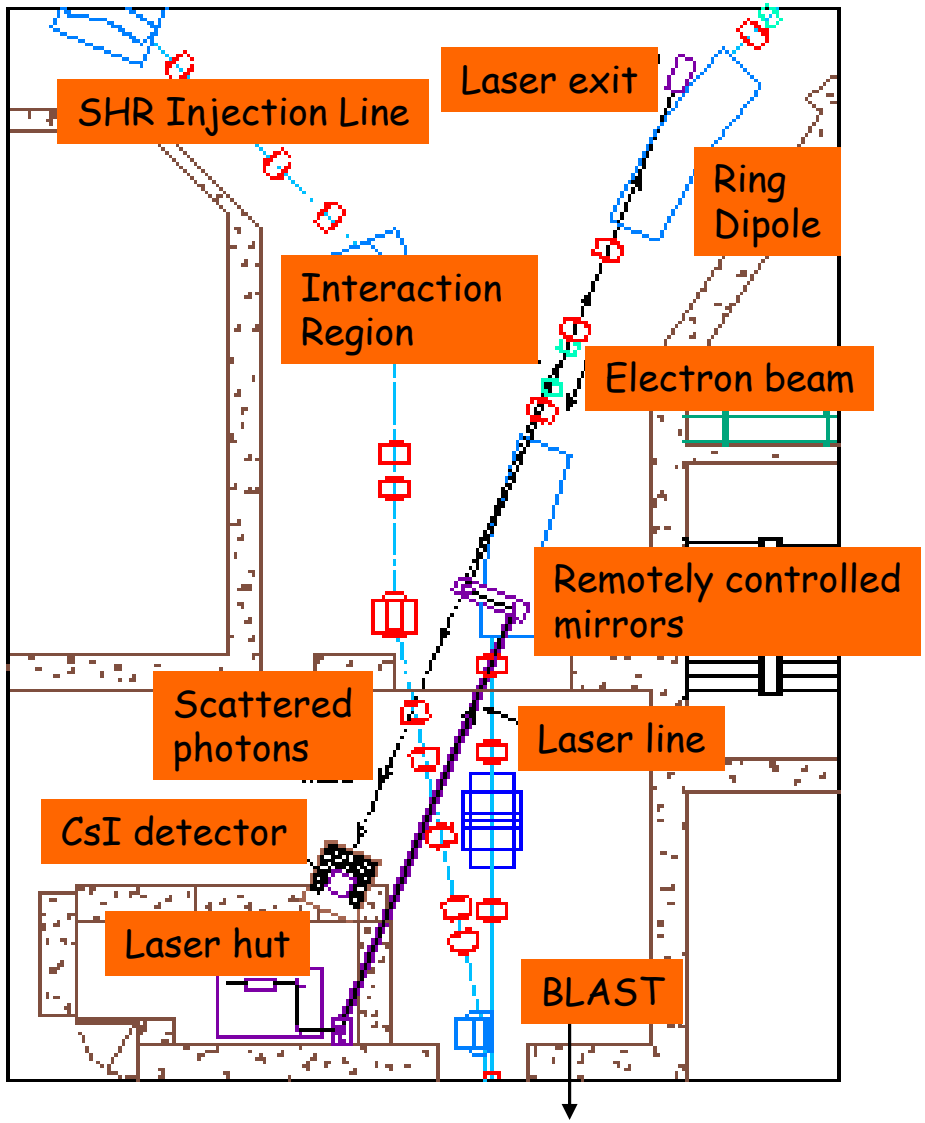

Scattered Gamma Ray Line

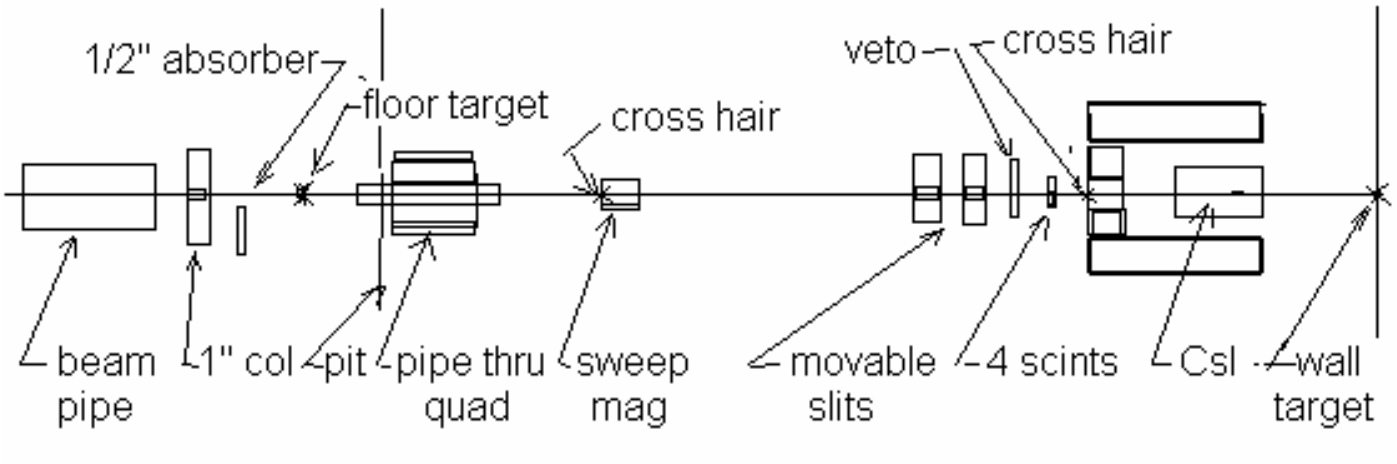

- Calorimeter detector located 10 *m* from exit window to reduce background
- Movable collimators used to eliminate background from beam halo
- Thin windows minimize attenuation of backscattered flux
- Sweep magnet, veto scintillator reject charged particles
- Scintillator hodoscope provides position information for beam alignment
- Pure CsI calorimeter offers resolution and speed for single photon mode
  - Gamma endpoint energy 25 MeV for 850 MeV electron beam
  - Transistorized PMT base gives linear response with very stable gain
- Variable thickness stainless steel absorbers used to regulate rate

Laser System

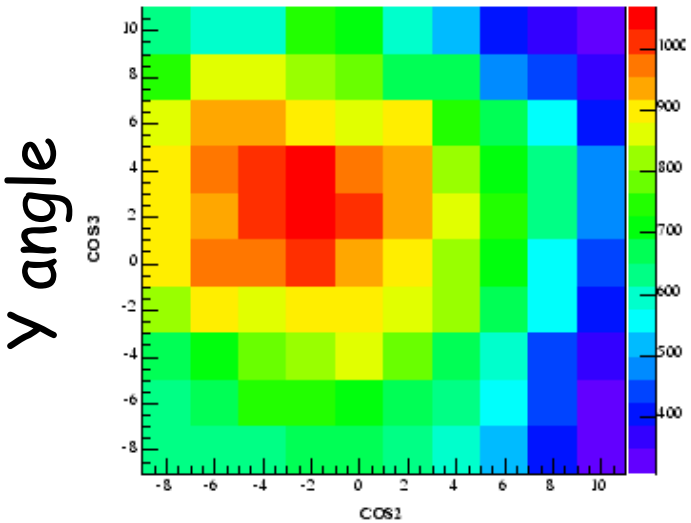

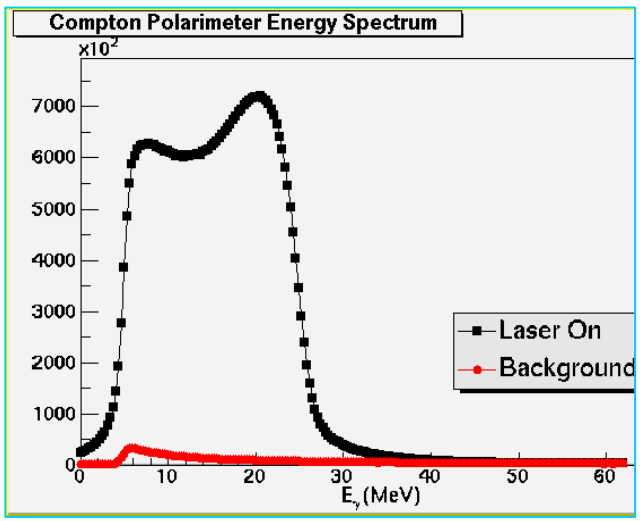

- Solid-state continuous-wave laser (5W output at 532 nm)
- Simple, robust lens arrangement for transport to IR and focusing
- Laser mechanically chopped by rotating wheel allowing background measurements (duty cycle adjustable)
- Circular polarization imparted by Helicity Pockels Cell (HPC) for rapid helicity reversal, measured periodically
- Phase-compensated mirror arrangement
- Final mirror inside vacuum system. Dipole chambers modified to allow laser to enter and exit IR above plane of beamline
- Multiple degrees of freedom for laser scans. Laser spatially constrained to intercept electron beam at angle < 2 *mrad*

High Intensity Operation

- Measurements made up to 190 mA. Stainless steel absorbers act as neutral density filter to control rate.
- Signal-to-background worsens at high currents as beam size increases, but still tractable
- Energy calibration stable on short time scale for high rates in CsI, gradual degradation with time

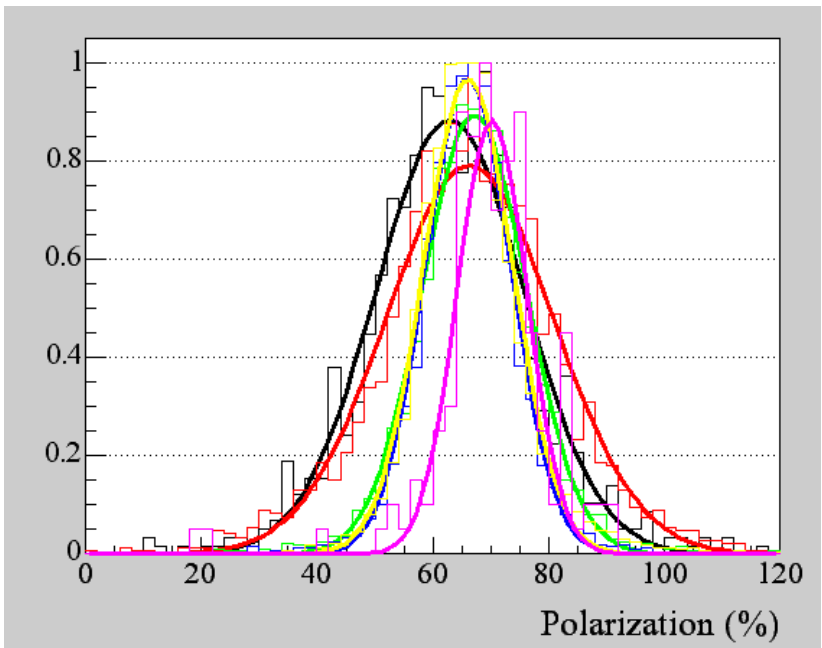

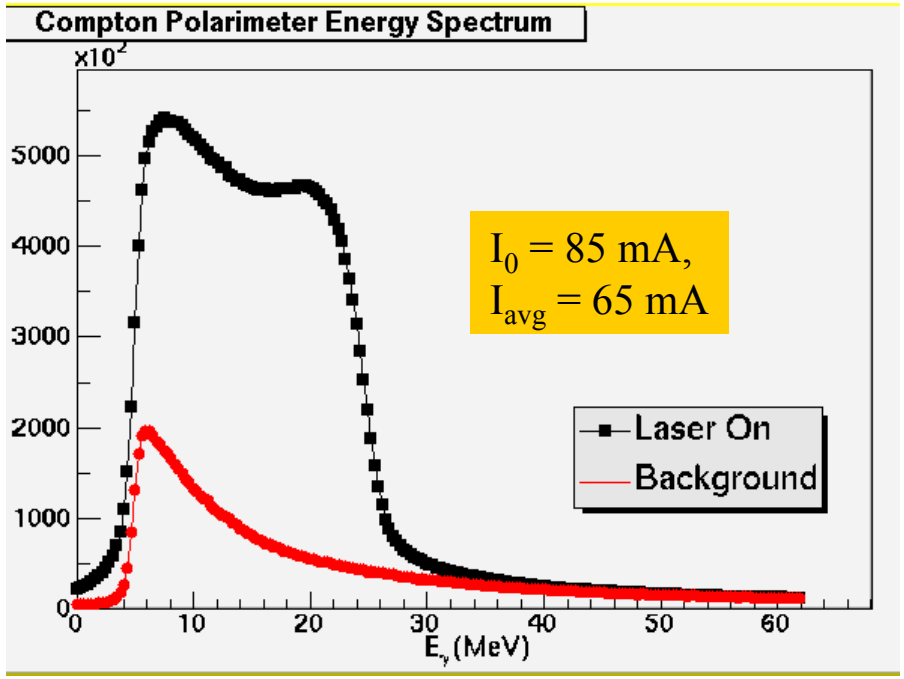

- Polarization reduction initially observed in going from low to higher currents. Loss found to be correlated with shifting of the beam tune and restored by retuning Ring.
- Small systematic correction to asymmetry for absorber thickness

Cumulative Results

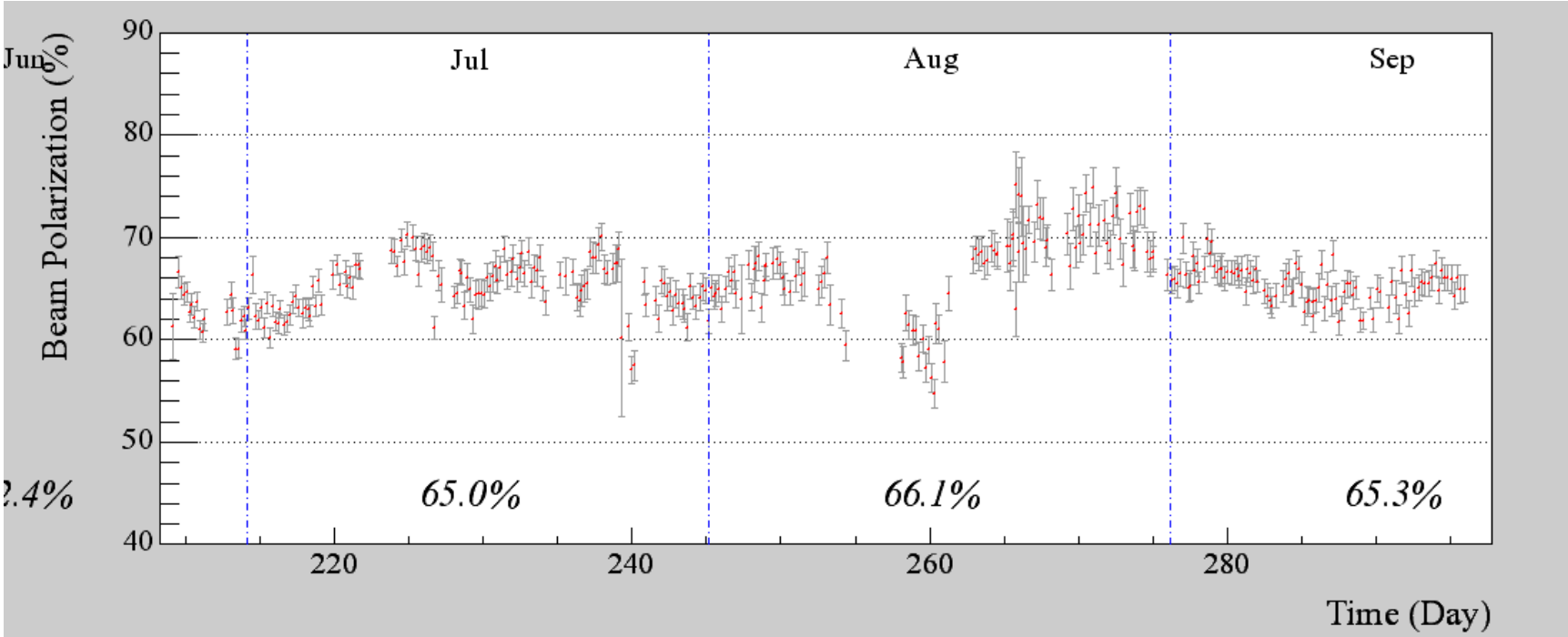

- Data stored in database of results for BLAST experiment in blocks of about 4 hours
- Polarization stable to within a few percent as a function of time. Changes usually correlated with beam properties.
- Mean polarization (2004): 0.663
- Mean polarization (July-Sep, 2004): 0.654
- Long term errors dominated by systematics

Atomic Beam Source (ABS)

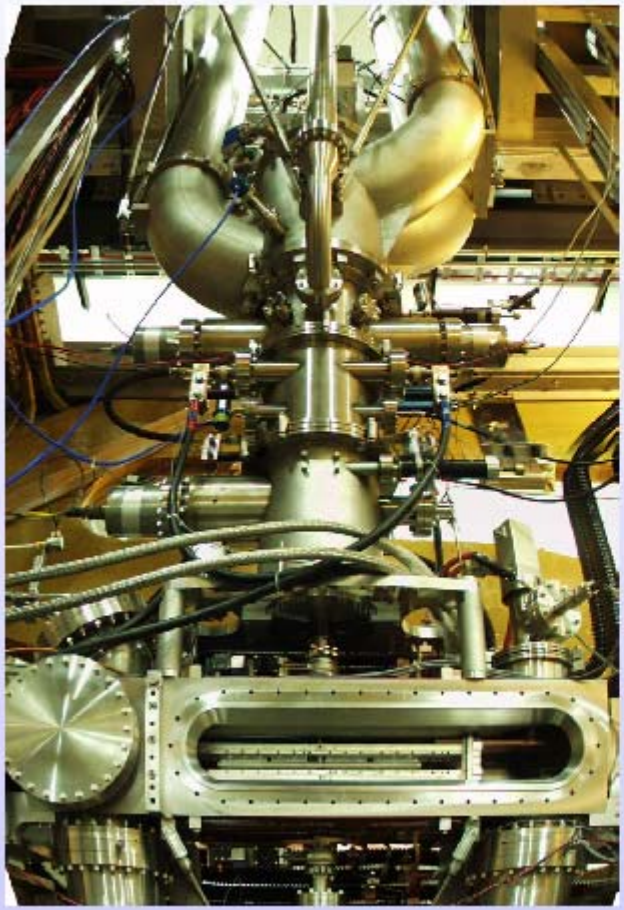

- Isotopically pure H or D
  Vector-polarized H
  Vector- and tensor-polarized D
- Target thickness / luminosity
  Flow 2.2×10^{16} atoms/s
  Density 6×10^{13} atoms/cm^2
  Luminosity 6×10^{31} cm^{-2}s^{-1}
- Target polarization typically 70-80%
  P_z, P_{zz} from analysis at low Q^2

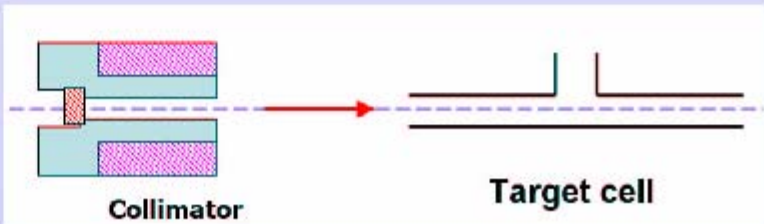

Atomic Beam Source

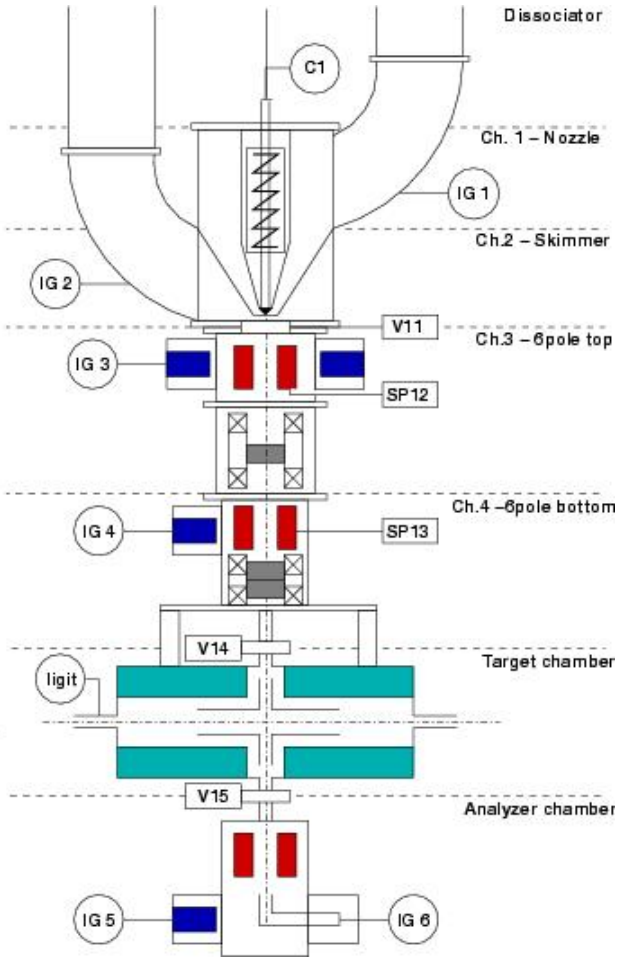

RF Dissociator

Sextupole System

RF Transition Units

Storage Cell

Breit-Rabi Polarimeter

Sextupole System

Used to focus atoms with pos. atomic electron spin and de-focus the rest.

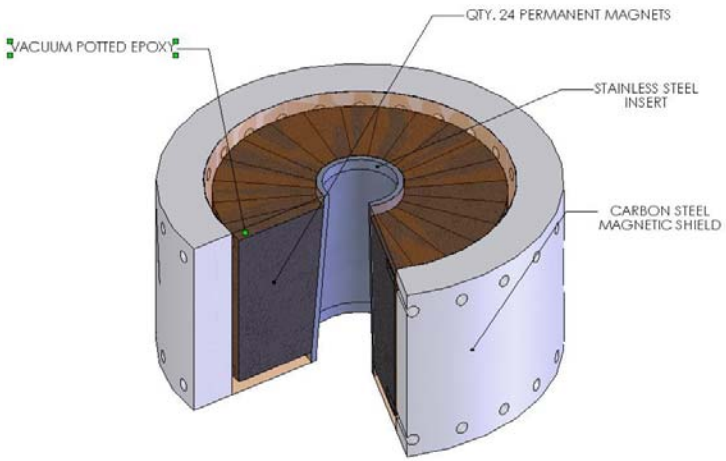

24 segments glued together.

Create radial field.

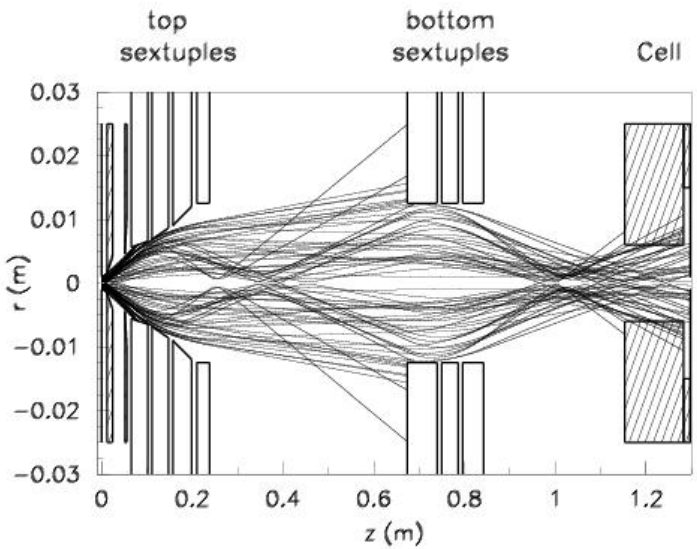

RAYTRACE simulations used to optimize location / opening of apertures, location of sextupoles.

Atomic Beam Source

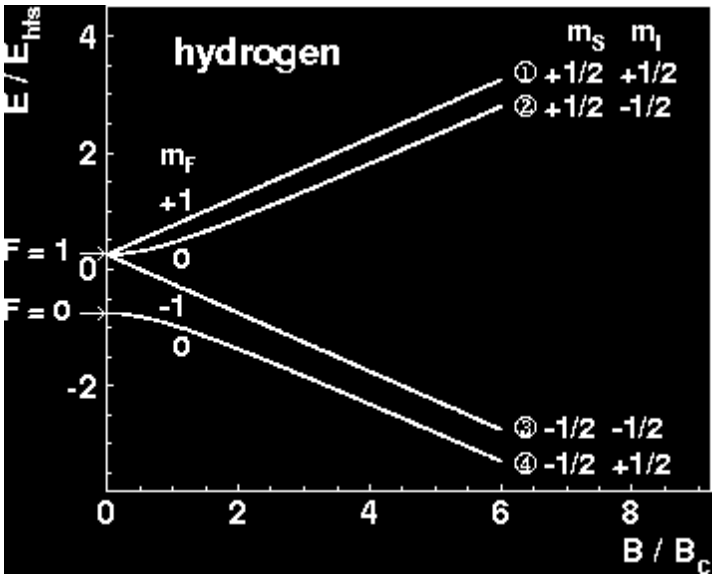

- Standard technology
- Dissociator & nozzle
- 2 sextupole systems
- 3 RF transitions

Spin State Selection:

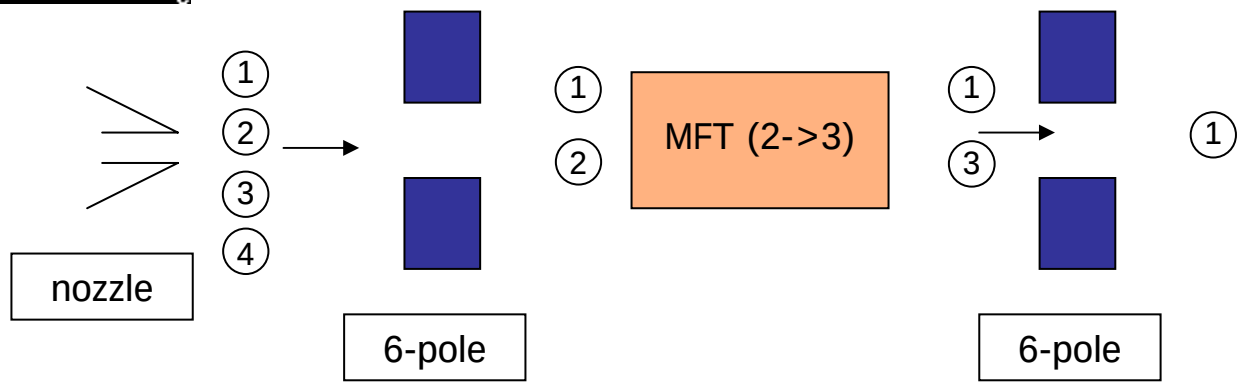

The Polarized ABS Target

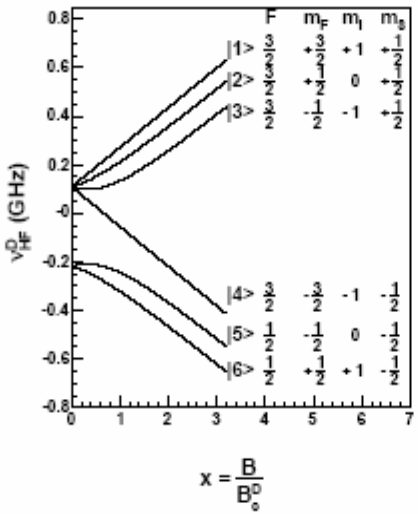

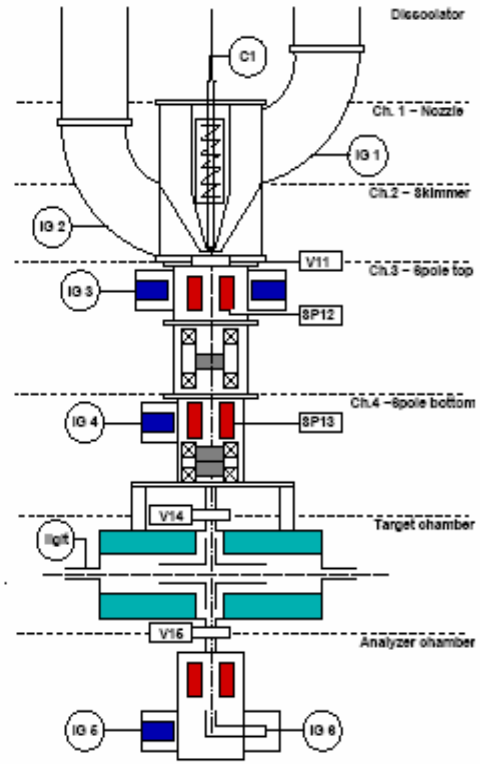

- RF dissociator produces atomic deuterium
- Sextupoles to select atomic states
- RF transitions to access nuclear polarizations
- Average Intensity $\sim$ $2.6 \times 10^{16}\ atoms \cdot s^{-1}$

RF Transition Units

To induce transitions between the hyperfine states.

MFT UNIT

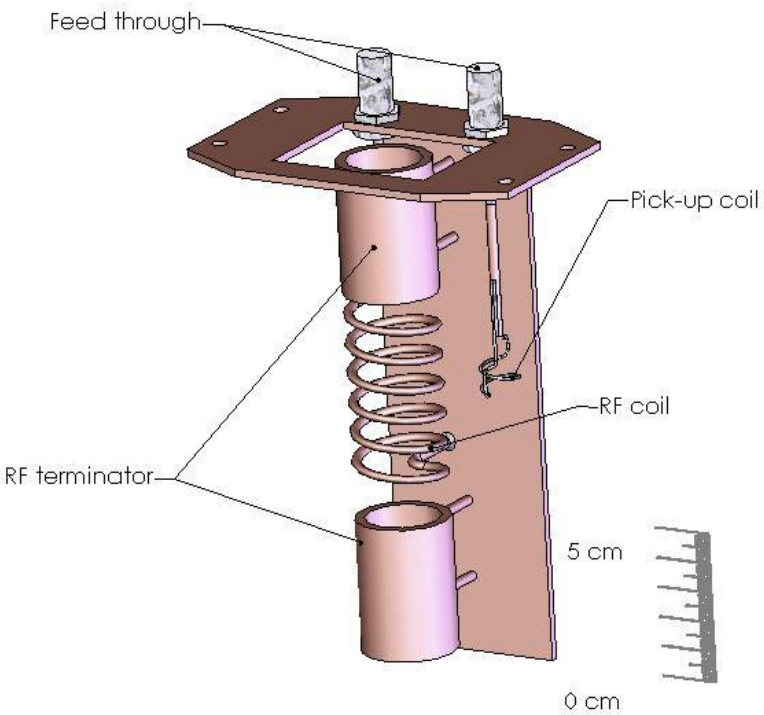

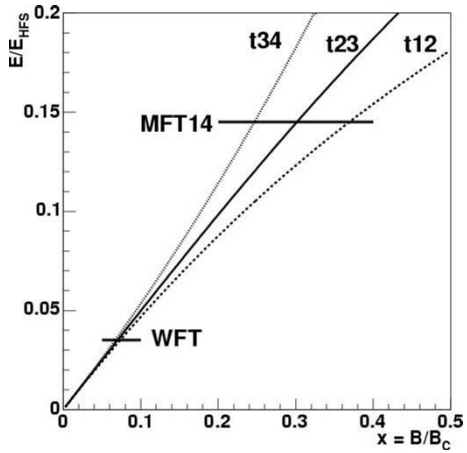

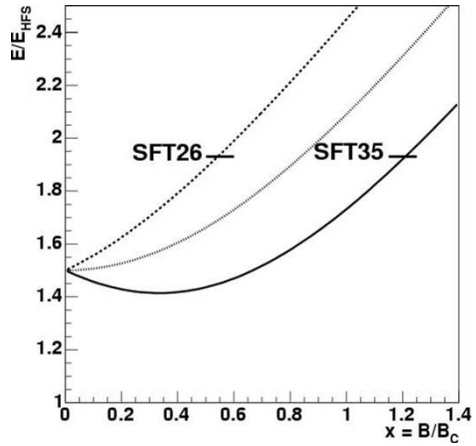

DEUTERIUM TRANSITIONS

MODE	Vector plus	Vector minus	Tensor minus
MFT	3-4	3-4	1-4
WFT	Off	1-4 and 2-3	Off
SFT	2-6	Off	3-5
P_e	0	0	0
P_z	+1	-1	0
P_{zz}	+1	+1	-2
B_{hold}	350G	350G	350G
n_{target}	1+6	3+4	2 +5

Deuterium Vector Polarization

$$\begin{pmatrix} n_1 \\ n_2 \\ n_3 \\ n_4 \\ n_5 \\ n_6 \end{pmatrix} \overset{6-pol}{\longrightarrow} \begin{pmatrix} n_1 \\ n_2 \\ n_3 \\ 0 \\ 0 \\ 0 \end{pmatrix} \overset{MFT}{\longrightarrow} \begin{pmatrix} n_1 \\ n_2 \\ 0 \\ n_4 \\ 0 \\ 0 \\ 0 \end{pmatrix} \overset{6-pol}{\longrightarrow} \begin{pmatrix} n_1 \\ n_2 \\ 0 \\ 0 \\ 0 \\ 0 \end{pmatrix} \overset{SFT}{\longrightarrow} \begin{pmatrix} n_1 \\ 0 \\ 0 \\ 0 \\ 0 \\ n_6 \end{pmatrix},$$

$$\begin{pmatrix} n_1 \\ n_2 \\ n_3 \\ n_4 \\ n_5 \\ n_6 \end{pmatrix} \overset{6-pol}{\longrightarrow} \begin{pmatrix} n_1 \\ n_2 \\ n_3 \\ 0 \\ 0 \\ 0 \end{pmatrix} \overset{MFT}{\longrightarrow} \begin{pmatrix} n_1 \\ n_2 \\ 0 \\ n_4 \\ 0 \\ 0 \\ 0 \end{pmatrix} \overset{6-pol}{\longrightarrow} \begin{pmatrix} n_1 \\ n_2 \\ 0 \\ 0 \\ 0 \\ 0 \end{pmatrix} \overset{WFT}{\longrightarrow} \begin{pmatrix} 0 \\ 0 \\ n_3 \\ n_4 \\ 0 \\ 0 \end{pmatrix},$$

Polarized Deuterium

- $S = 1, \quad M_S = \pm 1, 0$
- Population numbers $N = N_+ + N_- + N_0$

$$n_+ = \frac{N_+}{N}, \quad n_- = \frac{N_-}{N}, \quad n_0 = \frac{N_0}{N}$$

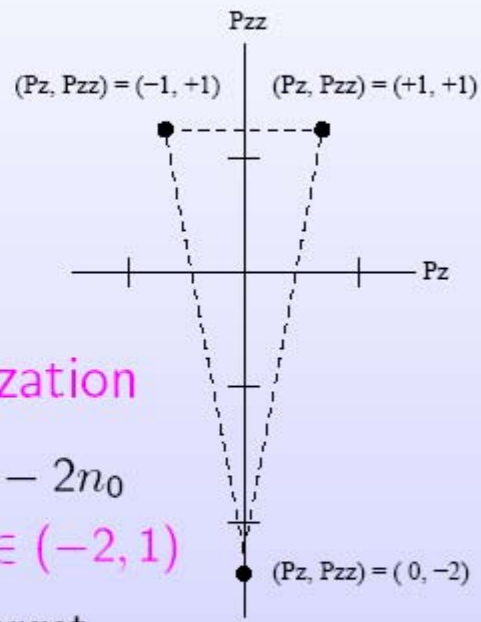

Vector polarization

$P_z = n_+ - n_- \in (-1, 1)$

S-state: $\vec{N}$-target

$\vec{\text{d}}(\vec{\text{e}},\text{e'n}) \rightarrow G_E^n / G_M^n$

$\vec{\text{d}}(\vec{\text{e}},\text{e'}) \rightarrow G_M^n$

$\vec{\text{d}}(\vec{\text{e}},\text{e'p}) \rightarrow A_{ed}^V$: D-state + FSI,MEC,IC,RC

Tensor polarization

$P_{zz} = n_+ + n_- - 2n_0 = 1 - 3n_0 \in (-2, 1)$

D-state: S=1-target

elastic $\rightarrow T_{20}, T_{21}, T_{22}$

$\overleftrightarrow{\text{d}}(\text{e},\text{e'p}) \rightarrow A_d^T$: D-state + FSI,MEC,IC,RC

Atomic Beam Source (ABS)

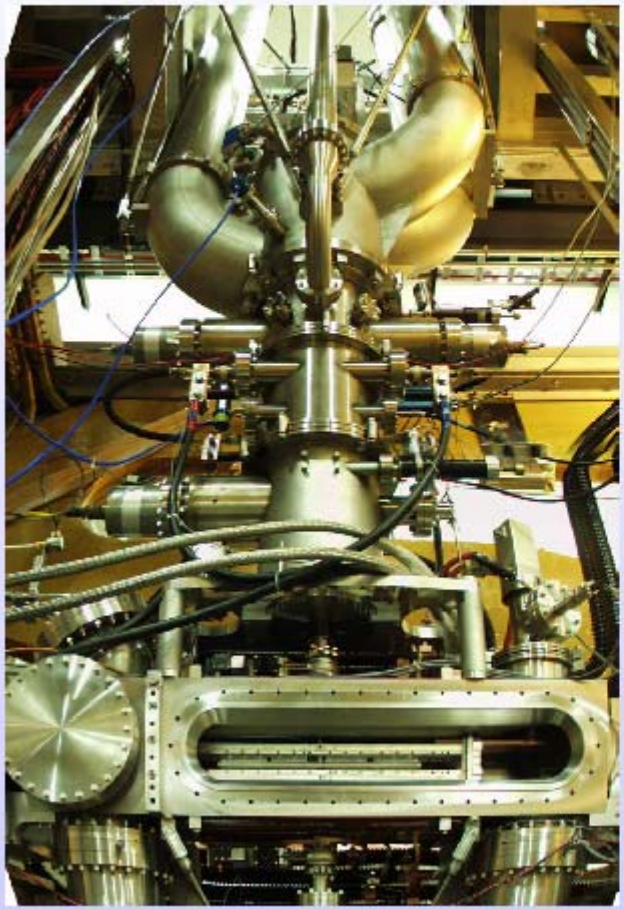

- Quasielastic $^2\vec{H}(\vec{e},e'p)$
- Beam-target asymmetry A_{ed}^V
- $A_{ed}^V(exp) = hP_z\ A_{ed}^V(th)$
- $< hP_z > = 0.558 \pm 0.009$,
  $< h > = 0.65 \pm 0.04$,
  $\rightarrow < P_z > = 0.86 \pm 0.05$

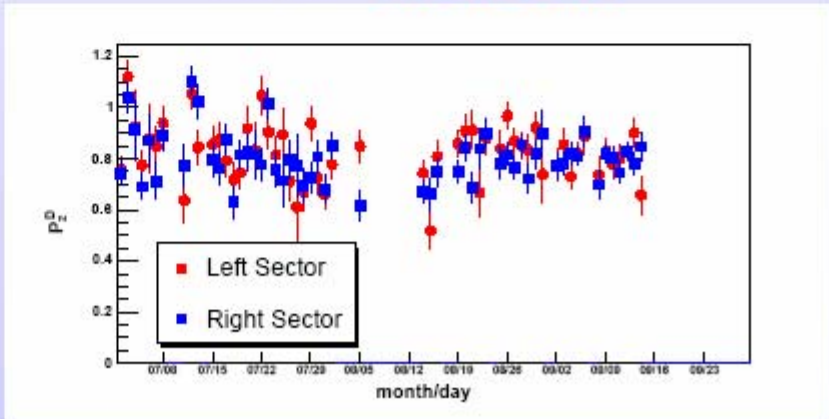

Atomic Beam Source (ABS)

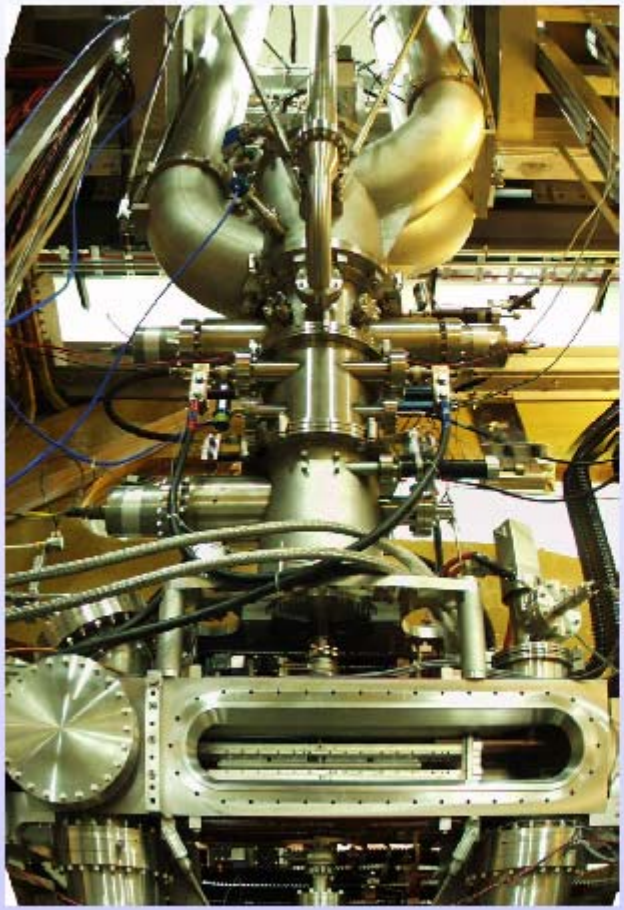

- Elastic $\overleftrightarrow{^2H}$(e,e'd)
- Tensor asymmetry A_d^T
- $A_d^T(\text{exp}) = P_{zz}\, A_d^T(\text{th})$
- $< P_{zz} > \; = 0.678 \pm 0.014$
- However: theory error 5–10%

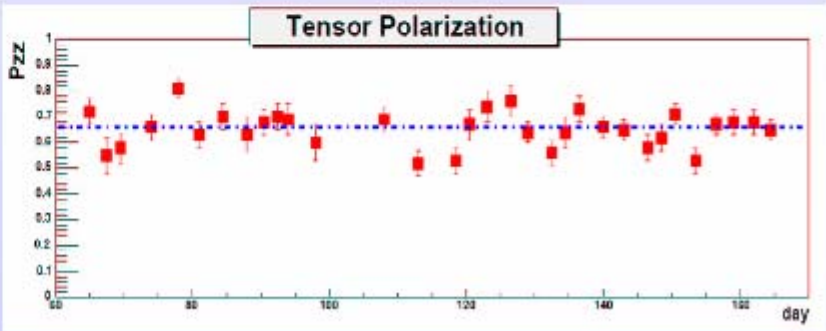

Storage Cell

Used to increase target thickness for internal target.

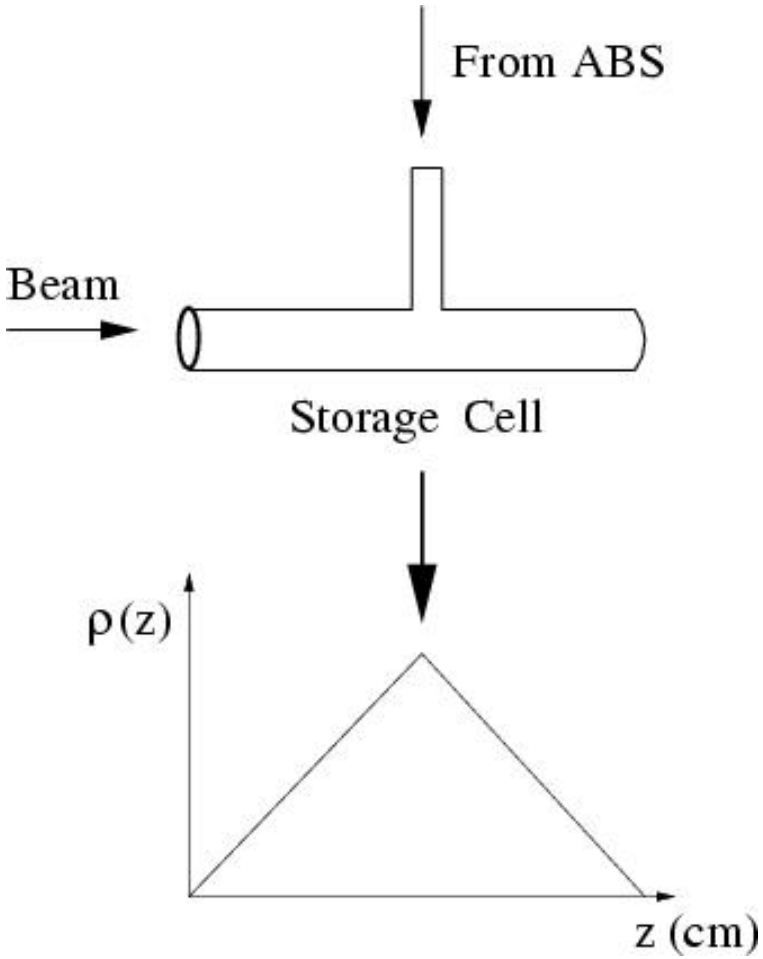

60 cm long, 15 mm diameter, Al.

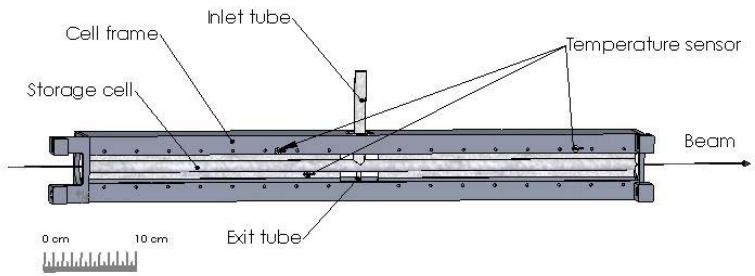

De-polarization effects:

Recombination

Spin Relaxation

To limit de-polarization:

Cooled to 100 K.

Coated with Dryfilm.

The BLAST Spectrometer

- Left-right symmetric detector
  - simultaneous parallel and perpendicular asymmetry determination
- Large acceptance
  - covers $0.1\text{GeV}^2 \leq Q^2 \leq 1\text{GeV}^2$
  - out-of-plane measurements

- DRIFT CHAMBERS
  - momentum determination, particle identification
- CERENKOV COUNTERS
  - electron/pion discrimination
- SCINTILLATORS
  - TOF, particle identification
- NEUTRON COUNTERS
  - neutron determination
- MAGNETIC COILS
  - 3.8kG toroidal field

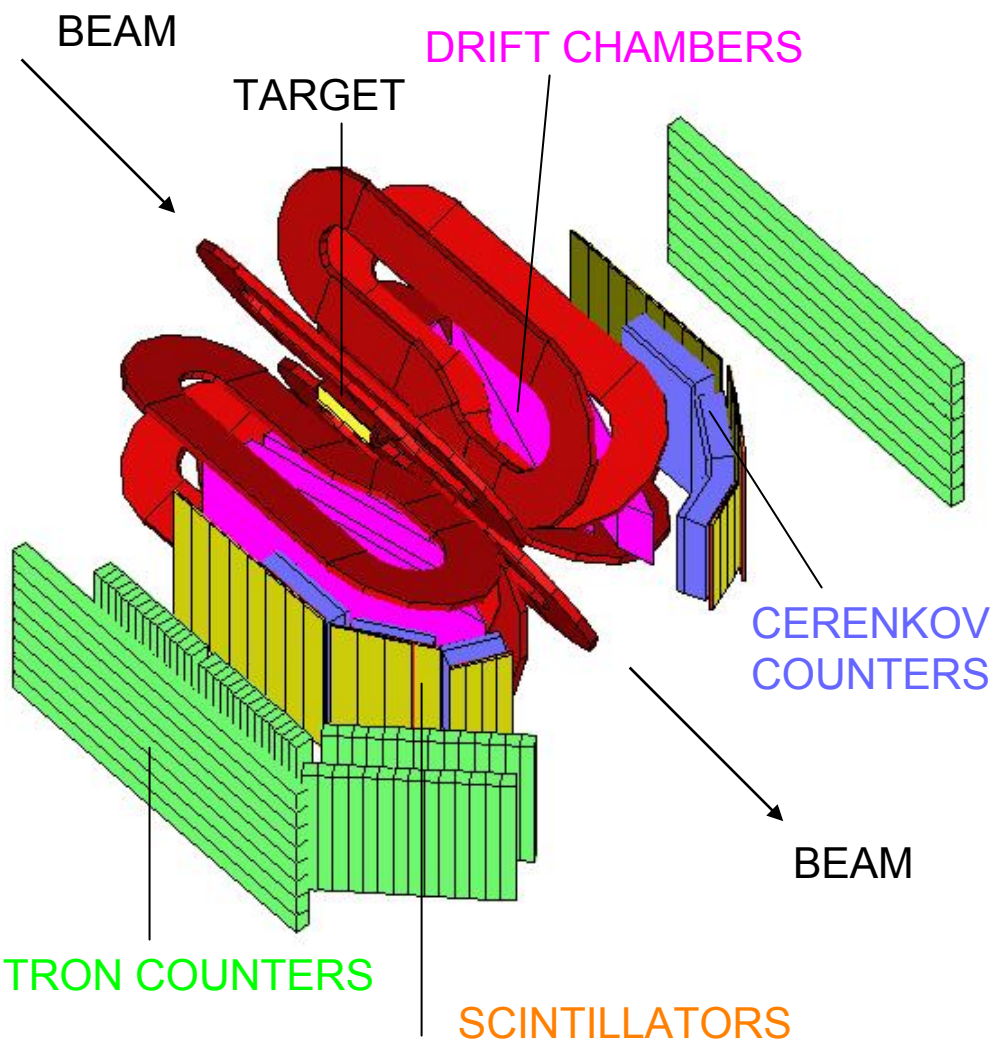

Experimental Layout

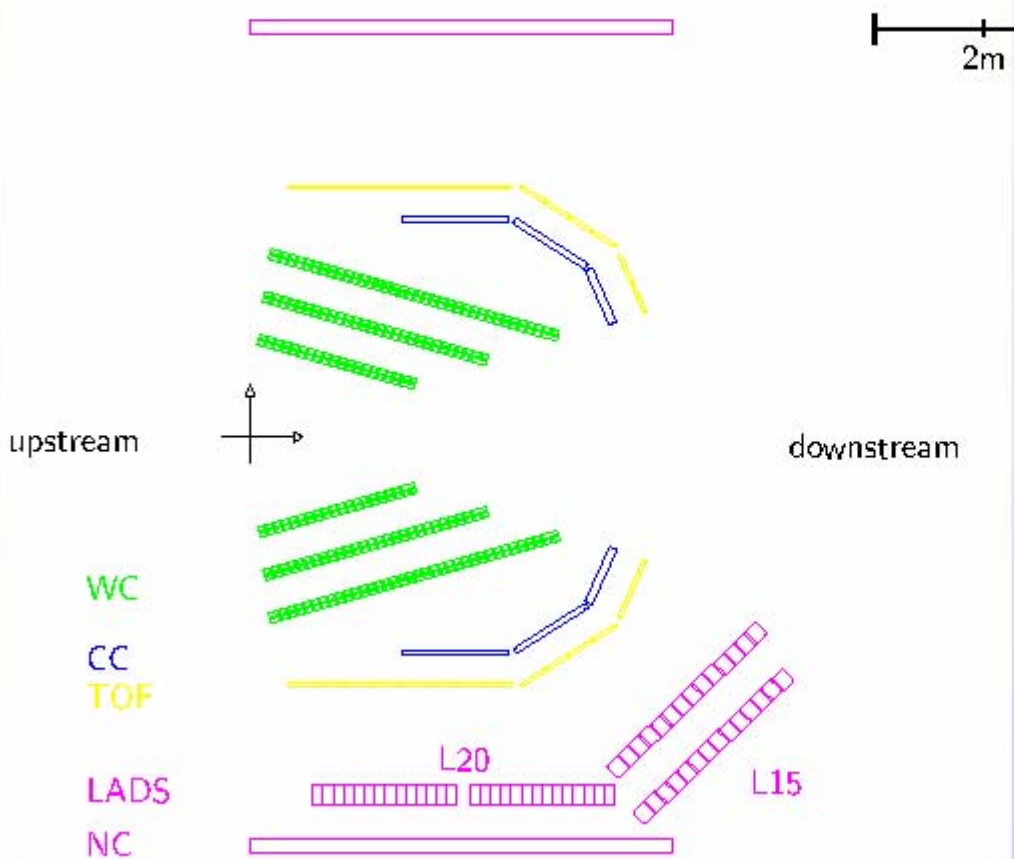

Parallel & Perpendicular Kinematics

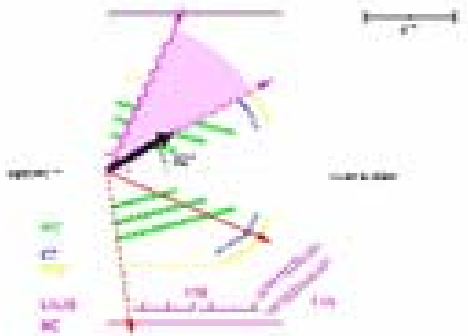

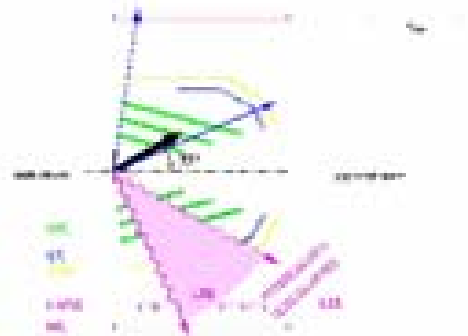

Parallel Kinematics:
Electron Right
$\vec{q}$ Left & $\sim \parallel \theta_T$

Perpendicular Kinematics:
Electron Left
$\vec{q}$ Right & $\sim \perp \theta_T$

Drift Chamber Design

- Three drift chambers in either detector sector
- Each chamber consists of two layers of drift cells
- Each drift cell consists of three sense wires

$$3 \times 2 \times 3 = 18 \text{ hits per track}$$

- ~1000 total sense wires
- ~9000 total field wires

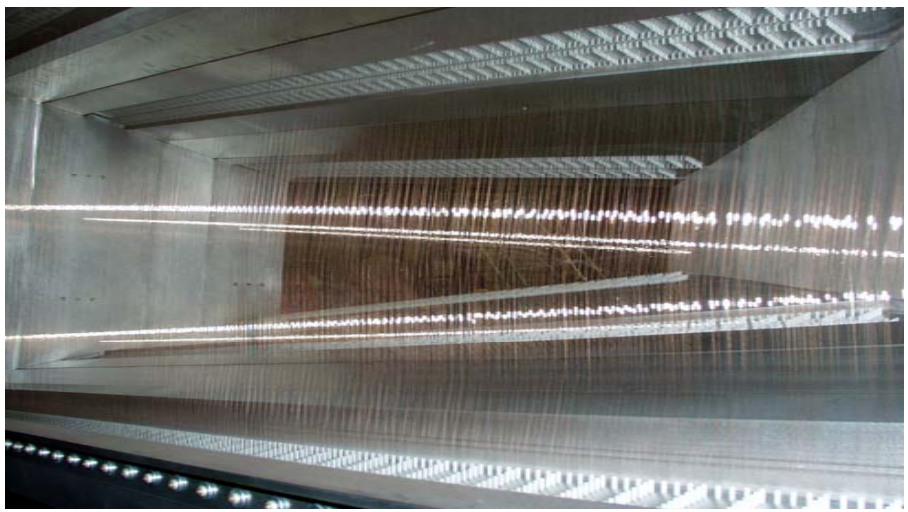

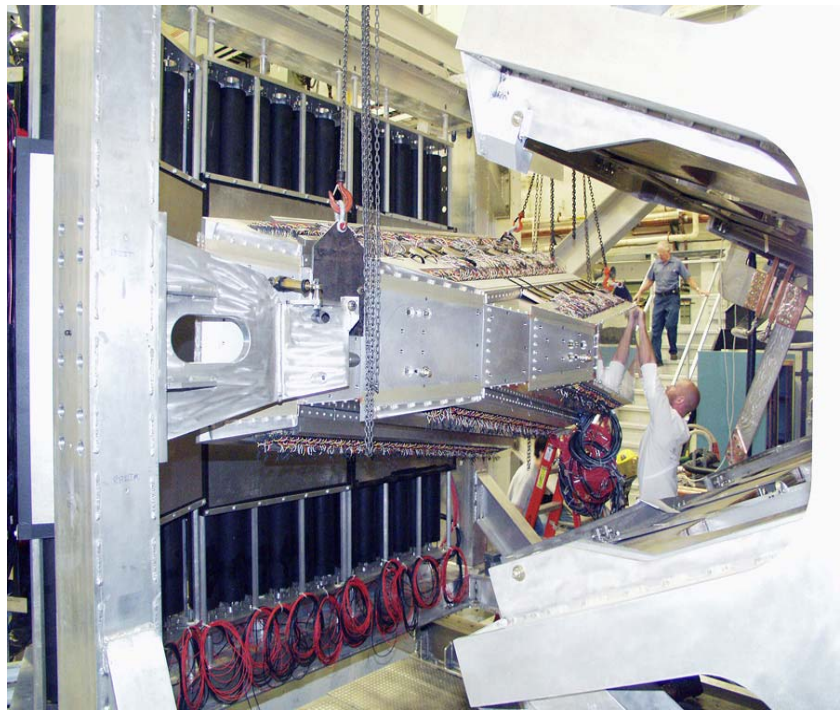

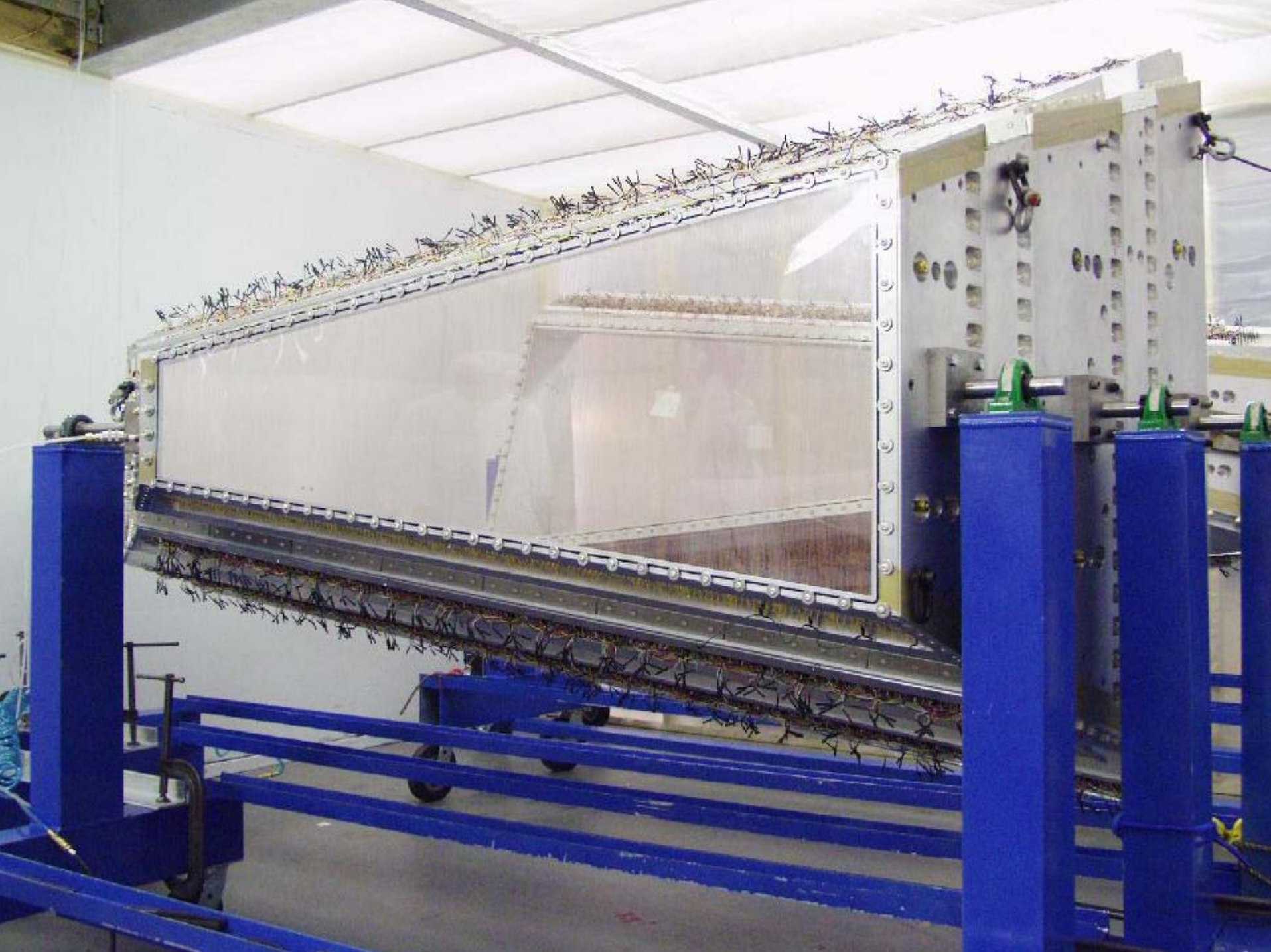

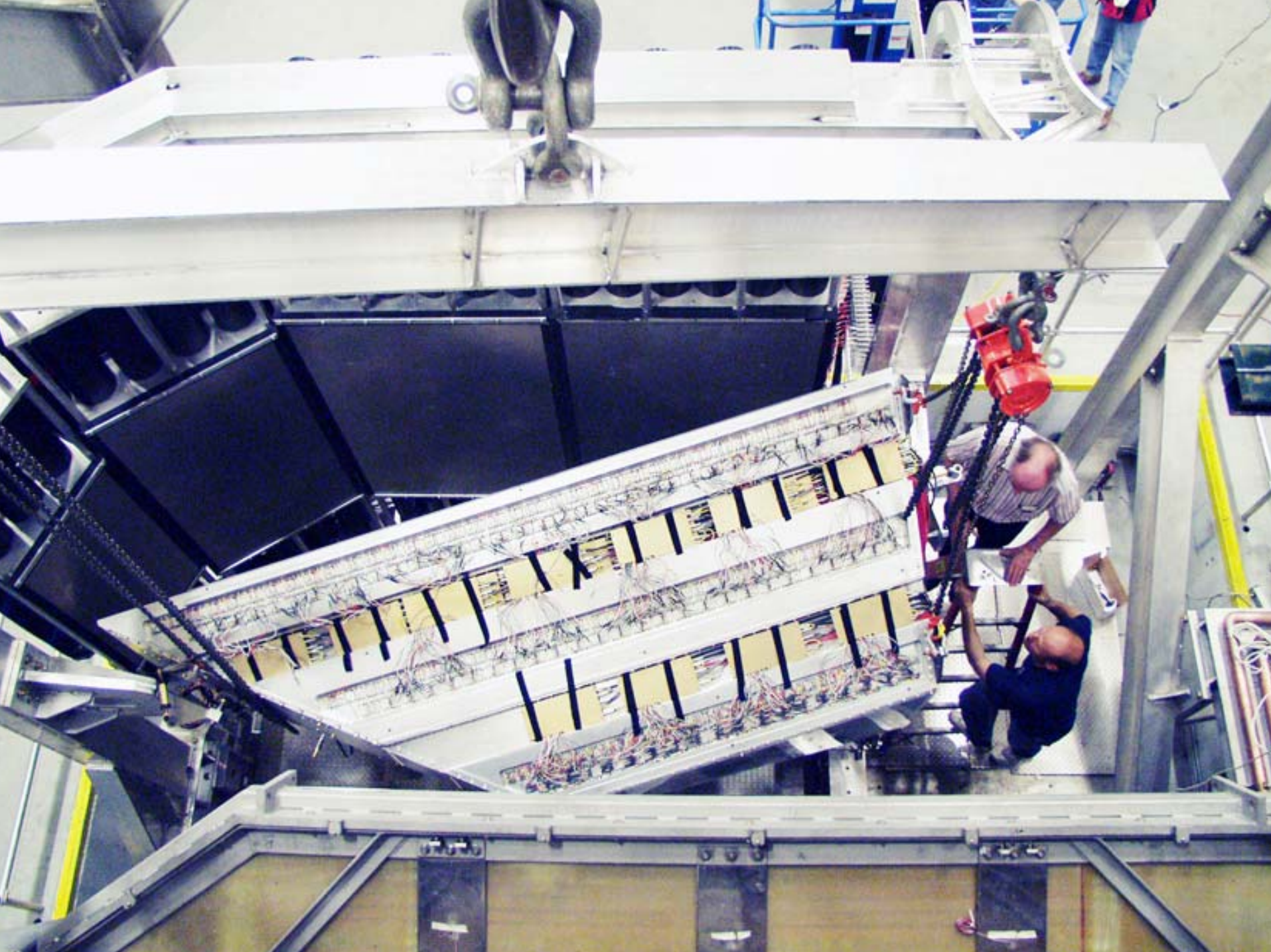

Wire Chambers

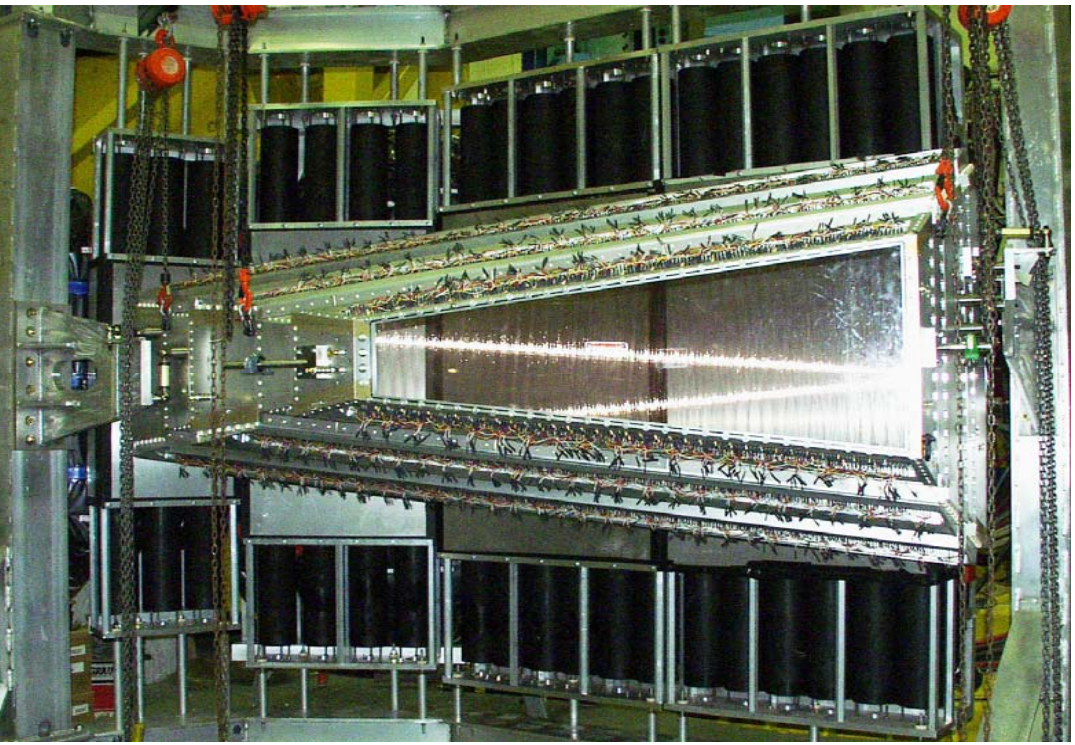

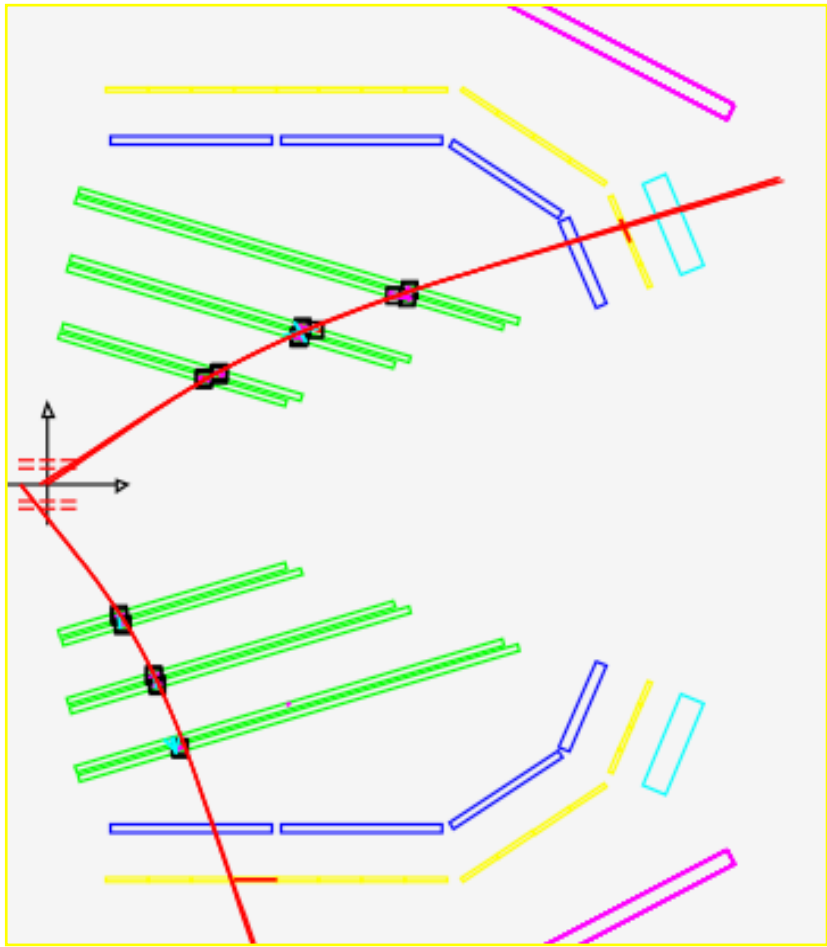

- 2 sectors × 3 chambers
- 954 sense wires
- resolution 200μm
- signal to noise 20:1

Drift Chamber Theory

- Apply uniform electric field
  - Function of HV wire setup
- Charged particles leave stochastic trail of ionized electrons
  - Series of accelerations and decelerations
- Electron amplification near readout wires (~10^5)
- Pulses → TDCs → distances
- Electrons "drift" to readout wires

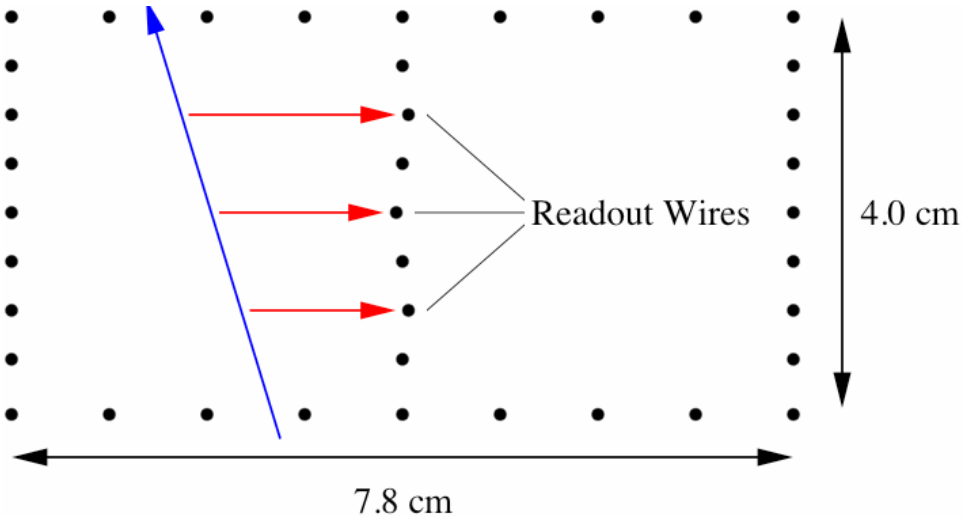

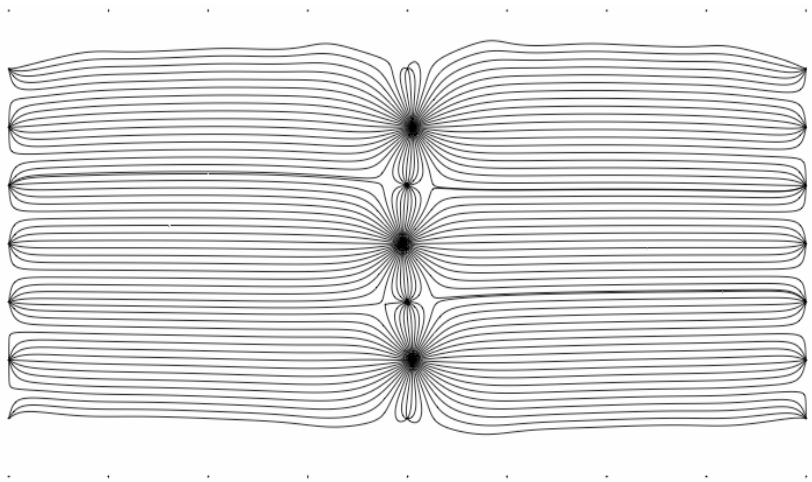

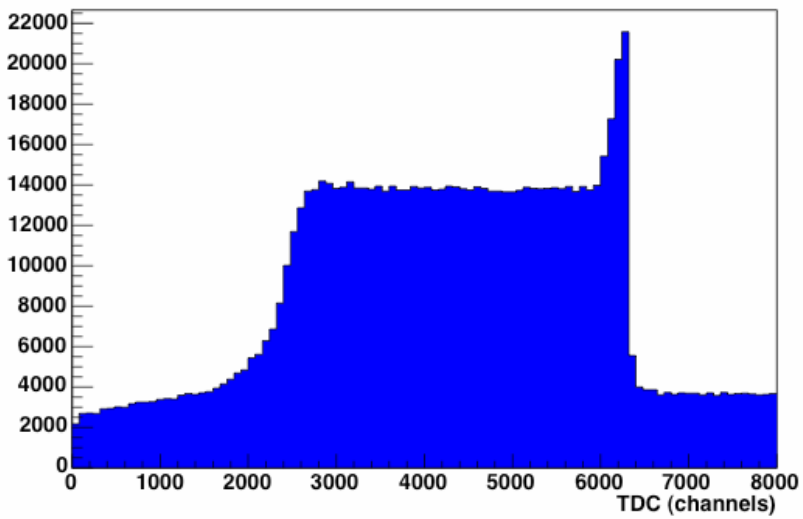

Time-of-Flight System

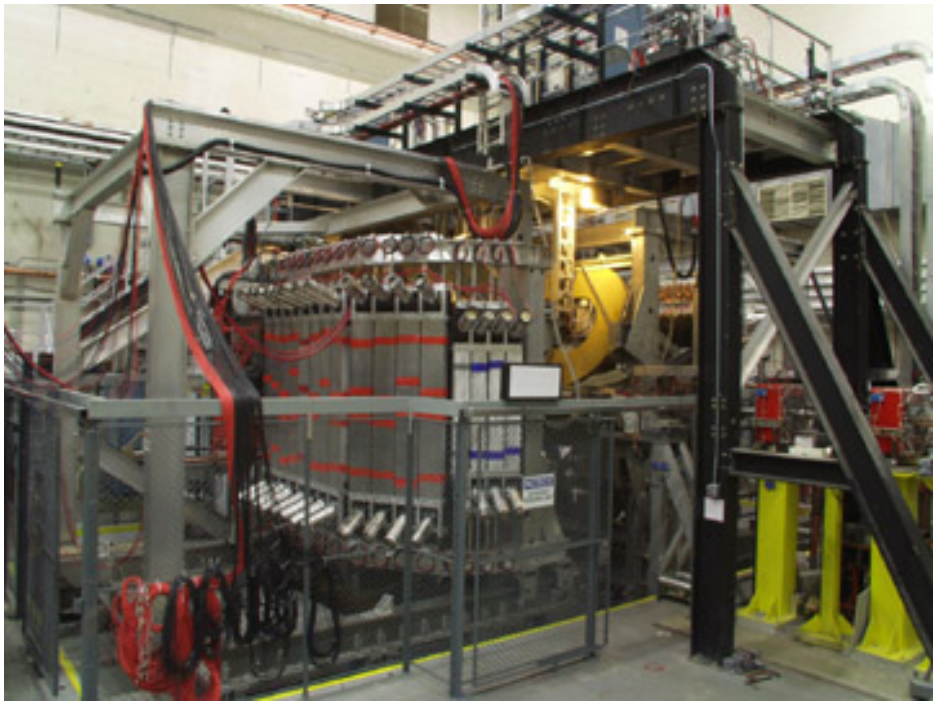

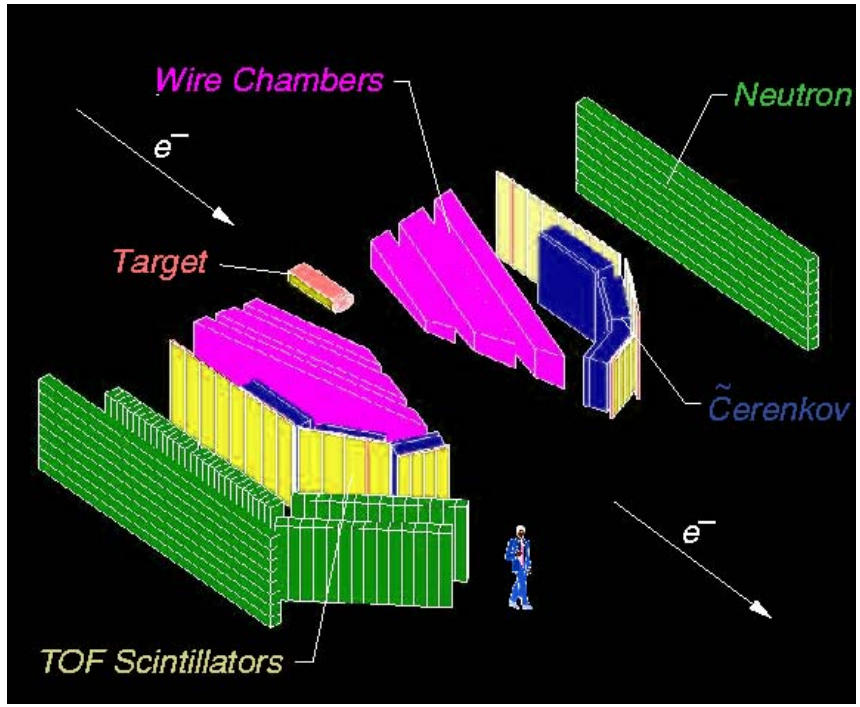

- scintillating material: BC-408 (Bicron)
- dimensions (cm):
  - backward angle: 180 - 26.10 - 2.54
  - forward angle: 120 - 17.8 - 2.54
- light-guides: BC-800
- optical adhesive: OP-21G (Dymax)

- 3” PMTs - 9822 (Electron Tubes)
- active (transistorized bases)
- optical grease: BC-630

Time-of-Flight Scintillators

- **Fast Timing Information**
  - TDC 50 $[ps/ch]$
  - Key to BLAST Trigger
- **Energy Information**
  - ADC 50 $[fC/ch]$
- **Performance**
  - $\delta_T < 500$ $[ps]$ $(FWHM)$
  - Efficiency $>$ 99%

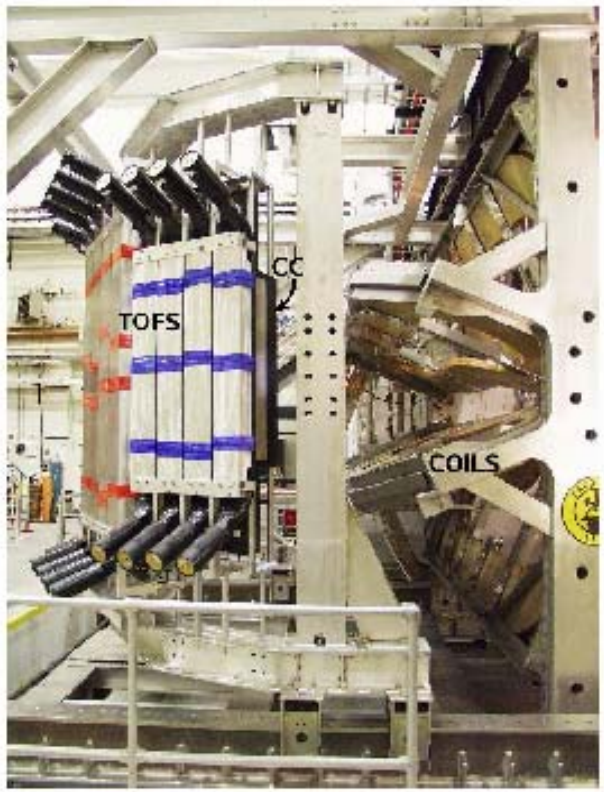

TOF Scintillators

- timing resolution: σ=350 ps
- velocity resolution: σ= 1%

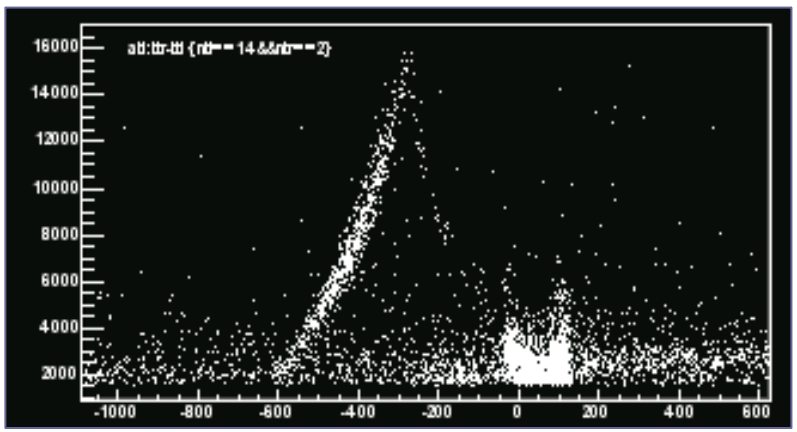

ADC spectrum

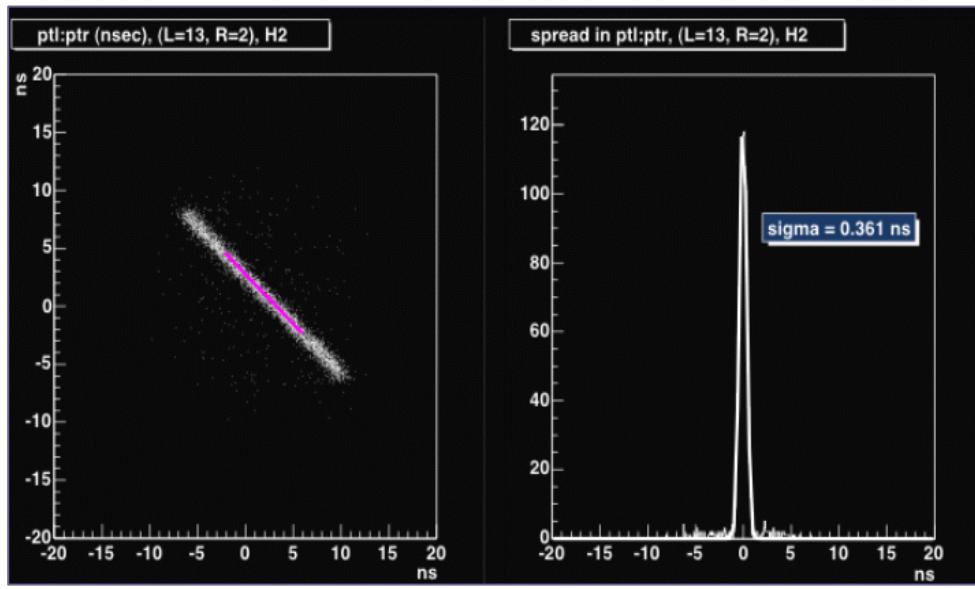

coplanarity cuts

Time-of-Flight System

- **Fast Timing Information**

  TDC – 50 ps/ch

  important for BLAST trigger

- **Energy Information**

- ADC – 50 fC/ch

- **Performance**

  efficiency > 99%

  δT < 500 ps FWHM

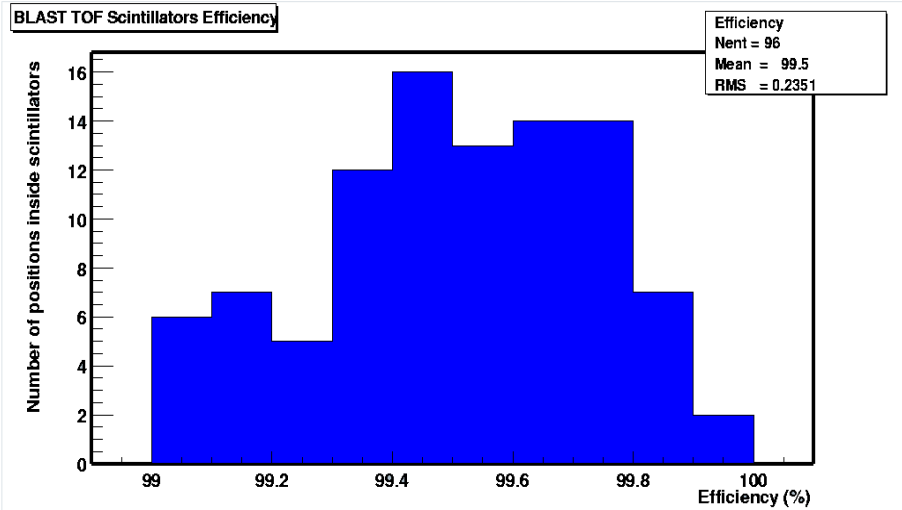

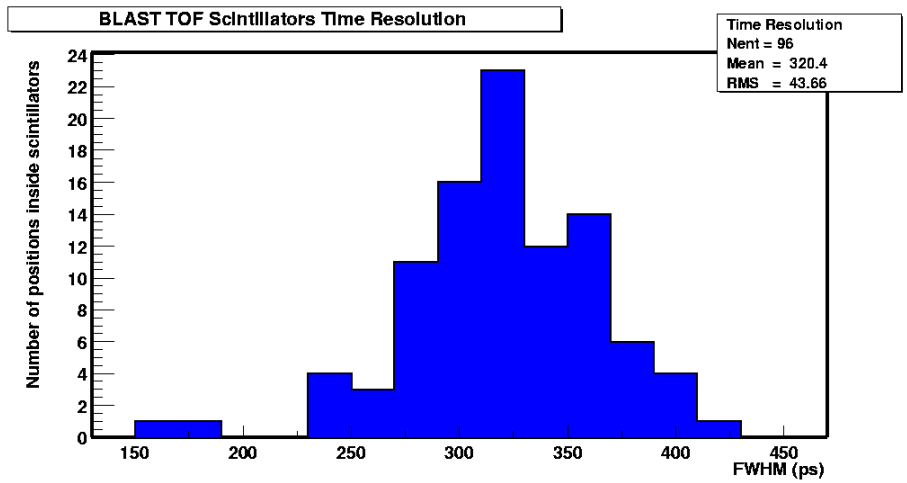

The BLAST Cherenkov Design

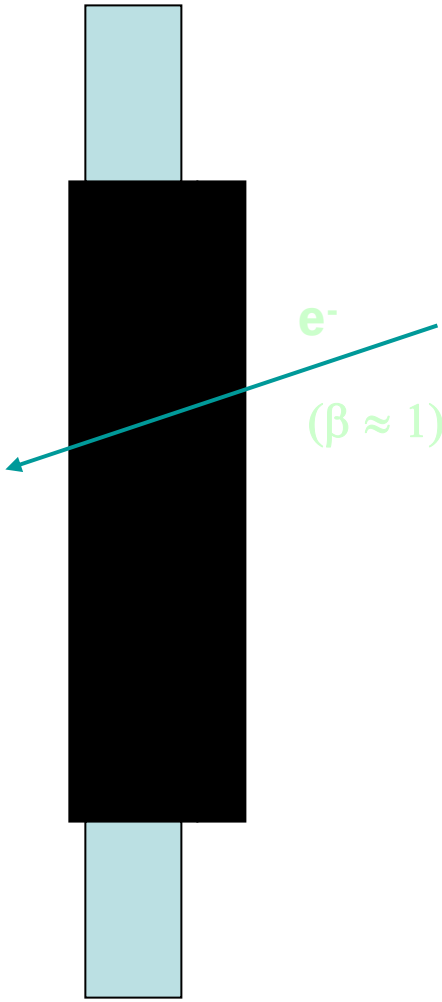

Requirements:

-
- >90% uniform efficiency
- compact, strong, low mass
- operate in magnetic field

Construction:

- clear **Aerogel** (Matsushita, Japan)

  index n=1.02 and 1.03

  thickness = 5cm and 7cm
- **Coating**: Diffusely Reflective Walls (LabSphere Inc.) (NH)
- PMTs: 5” Photonis (France) model XP4500B

  sensitive to 0.5 G
- **Boxes**: ASU machine shop

Simulations:

4-5 photoelectrons / 1 particle (β ≈ 1)

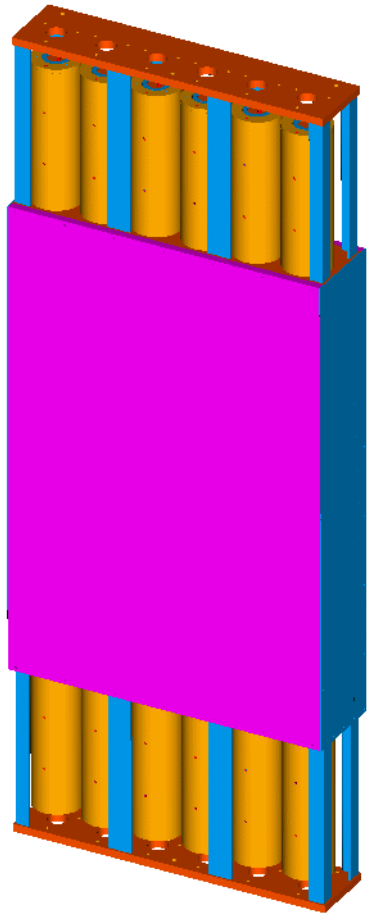

150cm x 100cm x 30cm

Čerenkov Detectors

- 1 cm thick aerogel tiles
- Refractive index 1.02-1.03
- White reflective paint
- 80-90 % efficiency

- 5" PMTs, sensitive to 0.5 Gauss
- Initial problems with B field
- Required additional shielding
- 50% efficiency without shielding

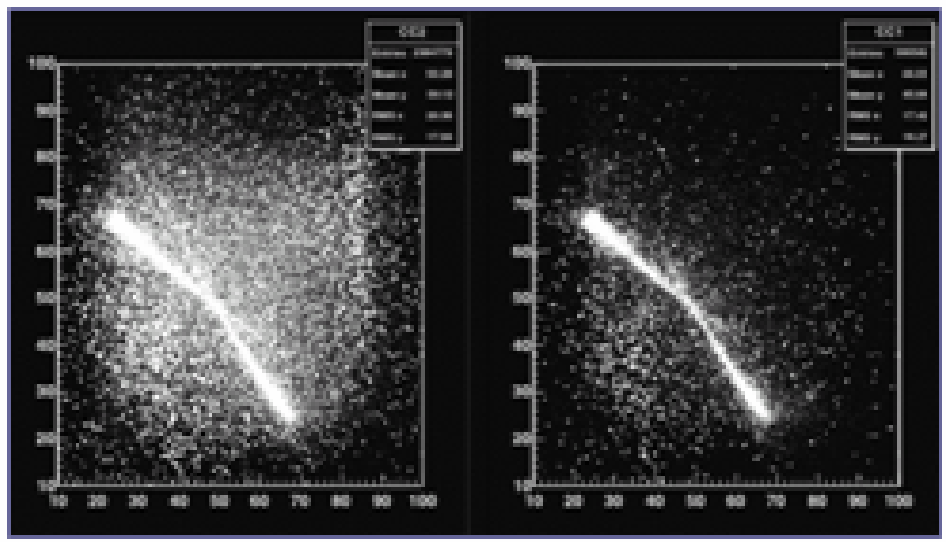

The BLAST Cherenkov Assembly

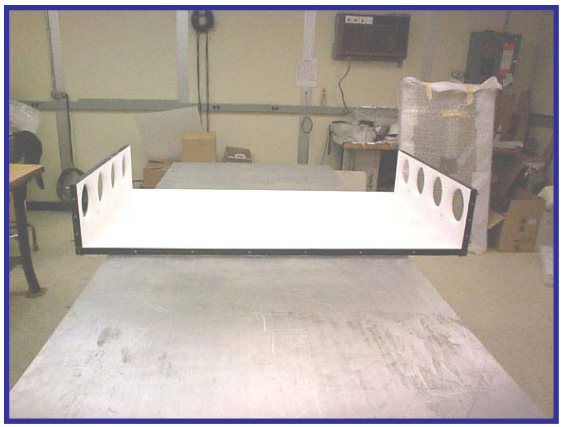

Top-Front Panels

Side Panels

PMT's Frames

PMT's Assemblies

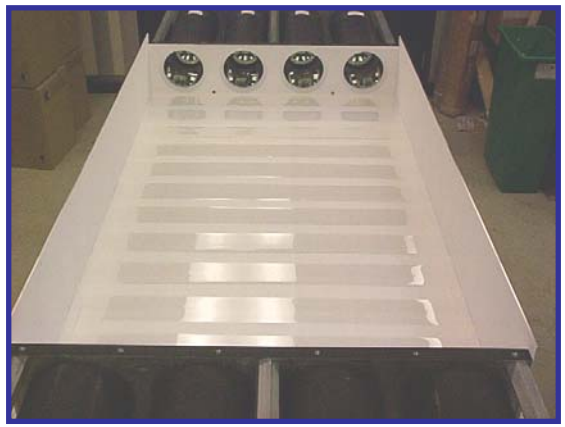

Aerogel Inside

Final Counter

Neutron Detectors

- Negatively charged track in coincidence with straight track that leaves no wire hits in the WC and no hit in TOF
- Enhanced detection in the right sector
- Ohio Wall and Large Acceptance Detector System, both plastic scintillators
- Average detection efficiency is ~30% in the right sector and ~10% in the left
- Cosmic events are used to calibrate neutron timing
- Time-walk correction is applied
- Flasher system is used to monitor timing shifts during the experiment

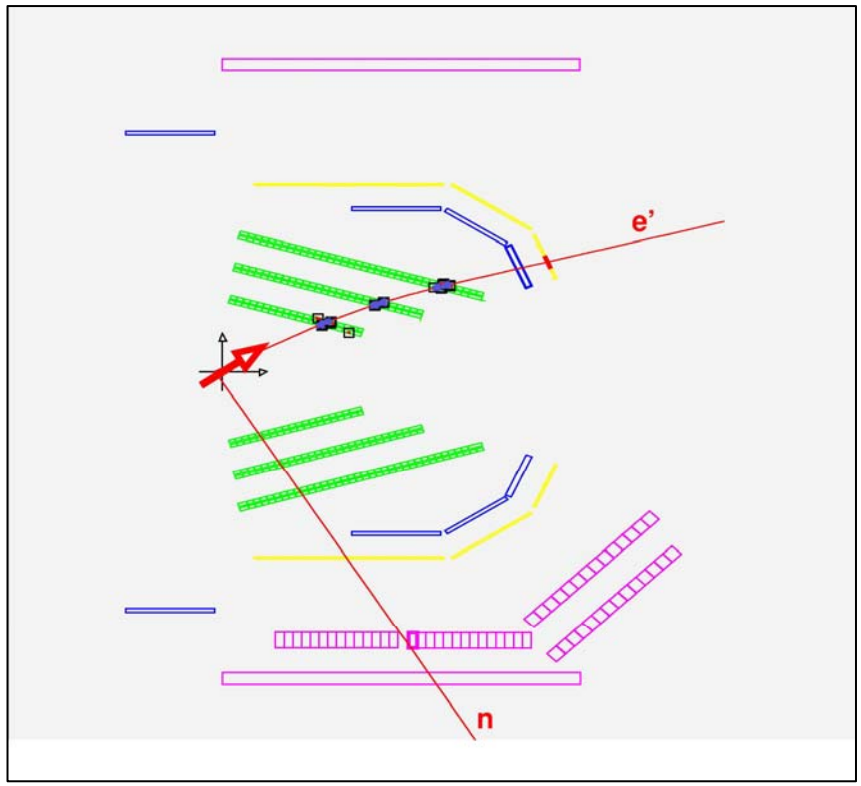

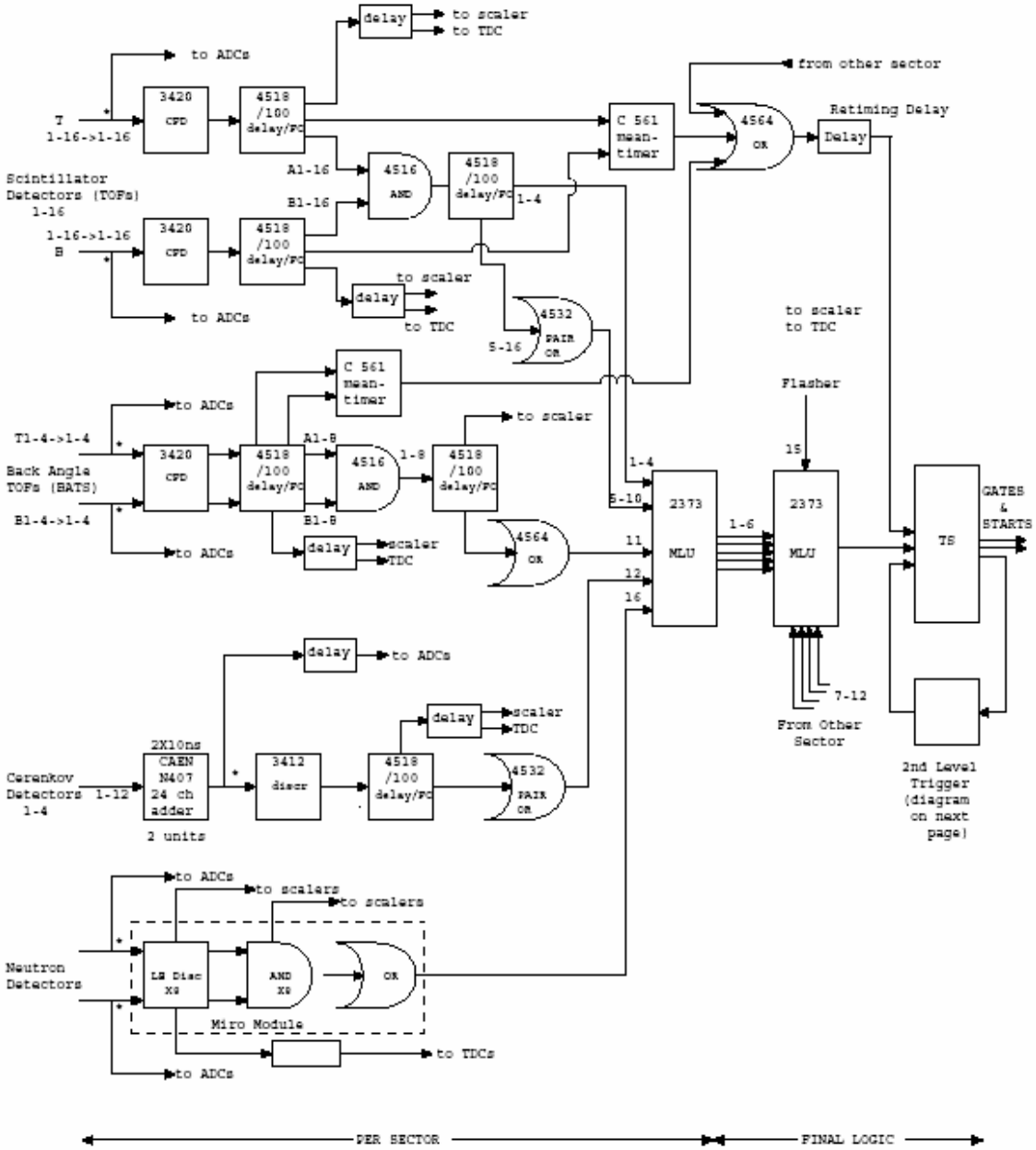

note: * all analog signal division in matched impedance passive splitters

- NIM & CAMAC electronics
- 16 bit sector MLU
- XMLU and Trigger Supervisor
- Fastbus TDCs and ADCs

BLAST Data Collection

- 3 MC integrated charge delivered to BLAST
- Programs for polarized hydrogen and vector/tensor-polarized deuterium
- Hydrogen run October-December 2004, spin angle 47°
  290 kC charge (90 pb^{-1}), P_z=82%
- Deuterium run May–October 2004, spin angle 32°
  450 kC charge (169 pb^{-1}), P_z=86%, P_{zz} = 68%
- Deuterium run March–May 2005, spin angle 47°
  550 kC charge (150 pb^{-1}), P_z=73%, P_{zz} = 56%
- Preliminary data presented for 2004 run (quasielastic) and for 2004+2005 runs (elastic)

Resolution and Yields

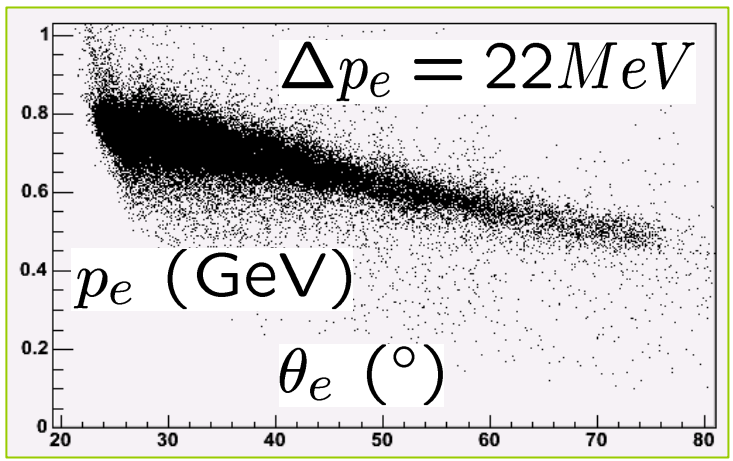

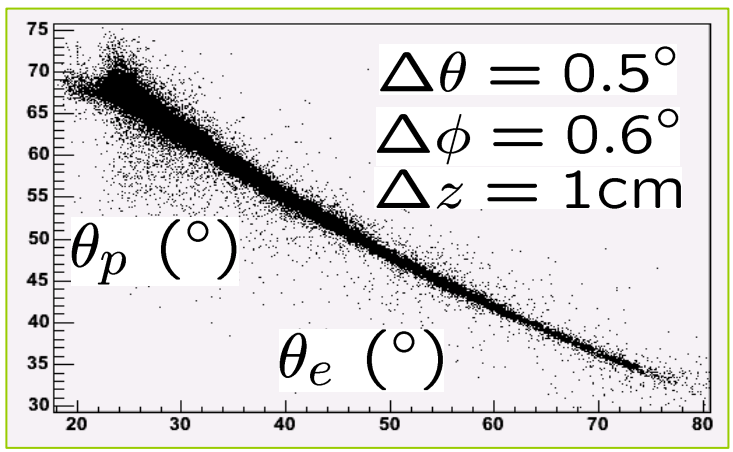

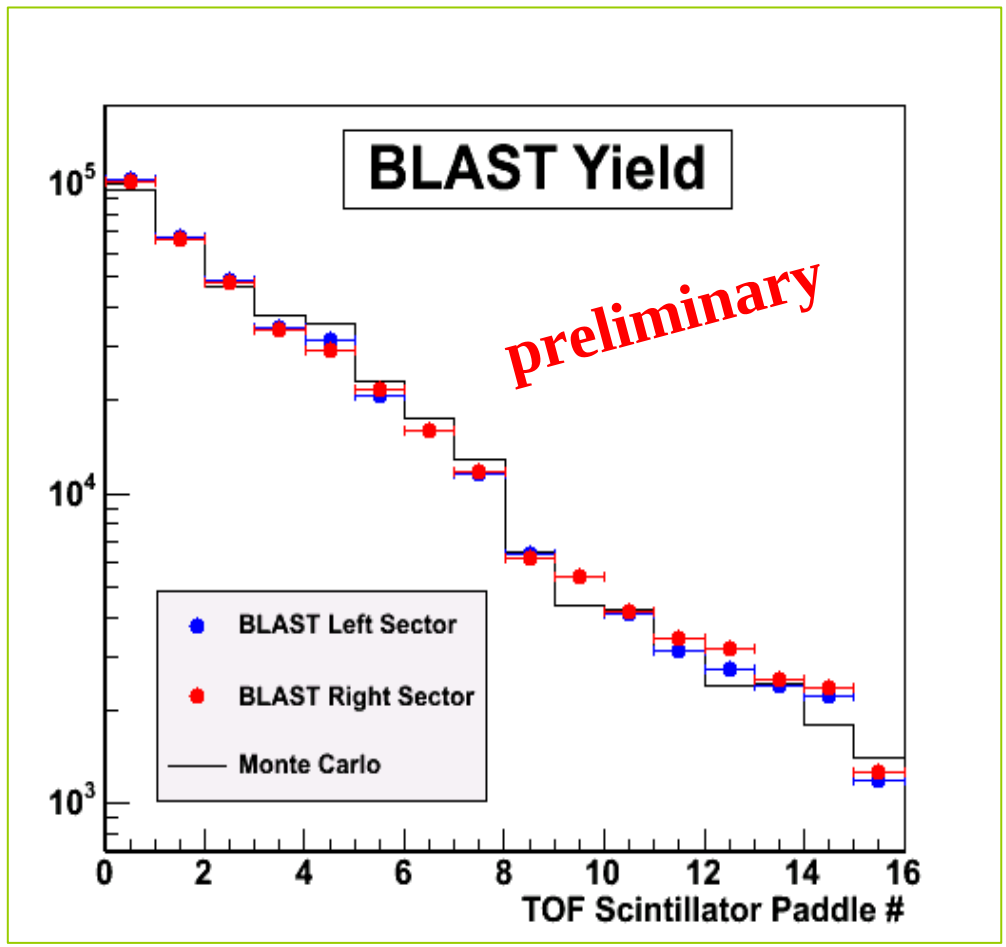

Detector Performance

- All detectors operating at or near designed level
  - Drift chambers ~98% efficient per wire
  - TOF resolution of 300ps
    - Clean event selection
  - Cerenkov counters 85% efficient in electron/pion discrimination
  - Neutron counters 10% (25-30%) efficient in left (right) sectors
    - To be improved further
- Reconstruction resolutions good but still being improved

	current	goal
σ_p	3%	2%
σ_θ	0.5°	0.3°
σ_ϕ	0.5°	0.5º
σ_z	1cm	1cm

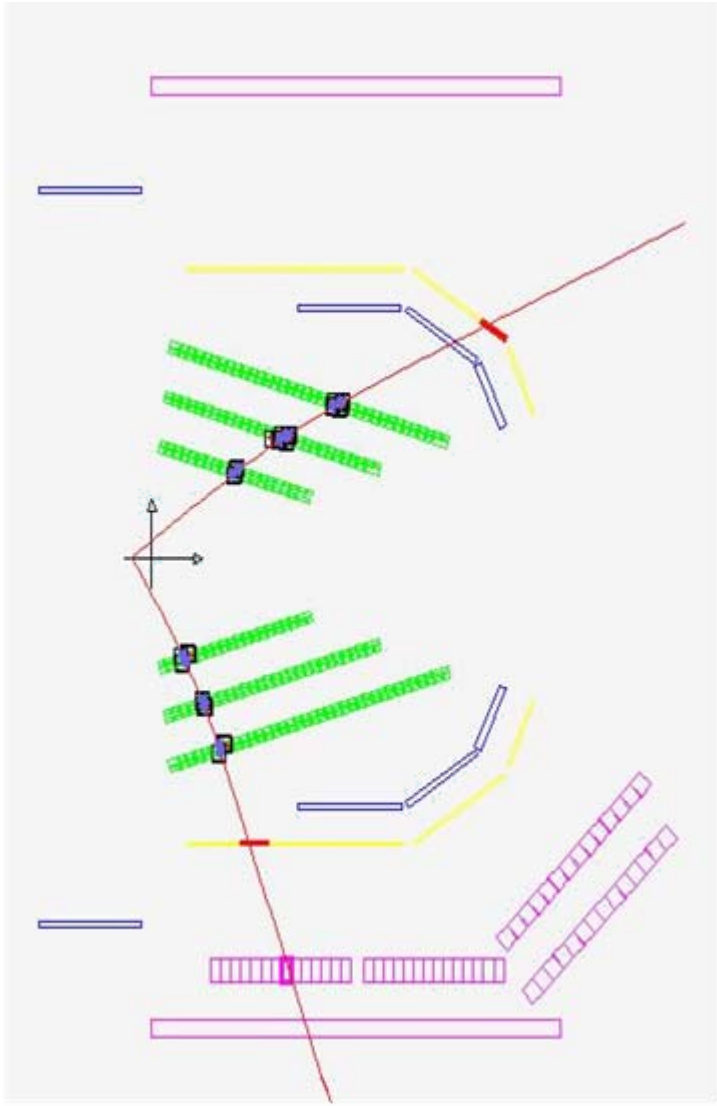

Introduction

Bates Large Acceptance Spectrometer Toroid

BLAST COLLABORATION

R. Alarcon, E. Geis, J. Prince, B. Tonguc, A. Young
Arizona State University, Tempe, AZ 85287

J. Althouse, C. D'Andrea, A. Goodhue, J. Pavel, T. Smith,
Dartmouth College, Dartmouth, NH

D. Dutta, H. Gao, W. Xu
Duke University Durham, NC 27708-0305

H. Arenhövel,
Johannes Gutenberg-Universität, Mainz, Germany

T. Akdogan, W. Bertozzi, T. Botto, M. Chtangeev, B. Clasie, C. Crawford,
A. Degrush, K. Dow, M. Farkhondeh, W. Franklin, S. Gilad, D. Hasell, E. Ilhoff, J. Kelsey,
M. Kohl, H. Kolster, A. Maschinot, J. Matthews, N. Meitanis, R. Milner, R. Redwine,
J. Seely, S. Sobczynski, C. Tschalaer, E. Tsentalovich, W. Turchinetz, Y. Xiao, C. Zhang, V. Ziskin, T. Zwart
Massachusetts Institute of Technology, Cambridge, MA 02139
and
Bates Linear Accelerator Center, Middleton, MA 01949

J. Calarco, W. Hersman, M. Holtrop, O. Filoti, P. Karpius, A. Sindile, T. Lee
University of New Hampshire, Durham, NH 03824

J. Rapaport
Ohio University, Athens, OH 45701

K. McIlhany, A. Mosser
United States Naval Academy, Annapolis, MD 21402

J. F. J. van den Brand, H. J. Bulten, H. R. Poolman
Vrije Universitaet and NIKHEF, Amsterdam, The Netherlands

W. Haeberli, T. Wise
University of Wisconsin, Madison, WI 53706